Data Assimilation Experiments of Radio Occultation Data using JMA Meso-4dvar System

-Impacts on the Heavy rainfall in Japan and the Development of Typhoon-

Hiromu SEKO*, Yoshinori SHOJI*, Masaru KUNII, and Toshitaka TSUDA*****

****Meteorological Research Institute, Japan Meteorological Agency***

*****University of Maryland***

****** Research Institute for Sustainable Humanosphere, Kyoto University***

Contents

1. Assimilation method of GPS radio occultation data.
2. Synergistic improvement of the heavy rainfall forecast using GPS RO data and ground-based GPS data.
3. Impacts on the development of typhoon USAGI (0705).
4. Summary.

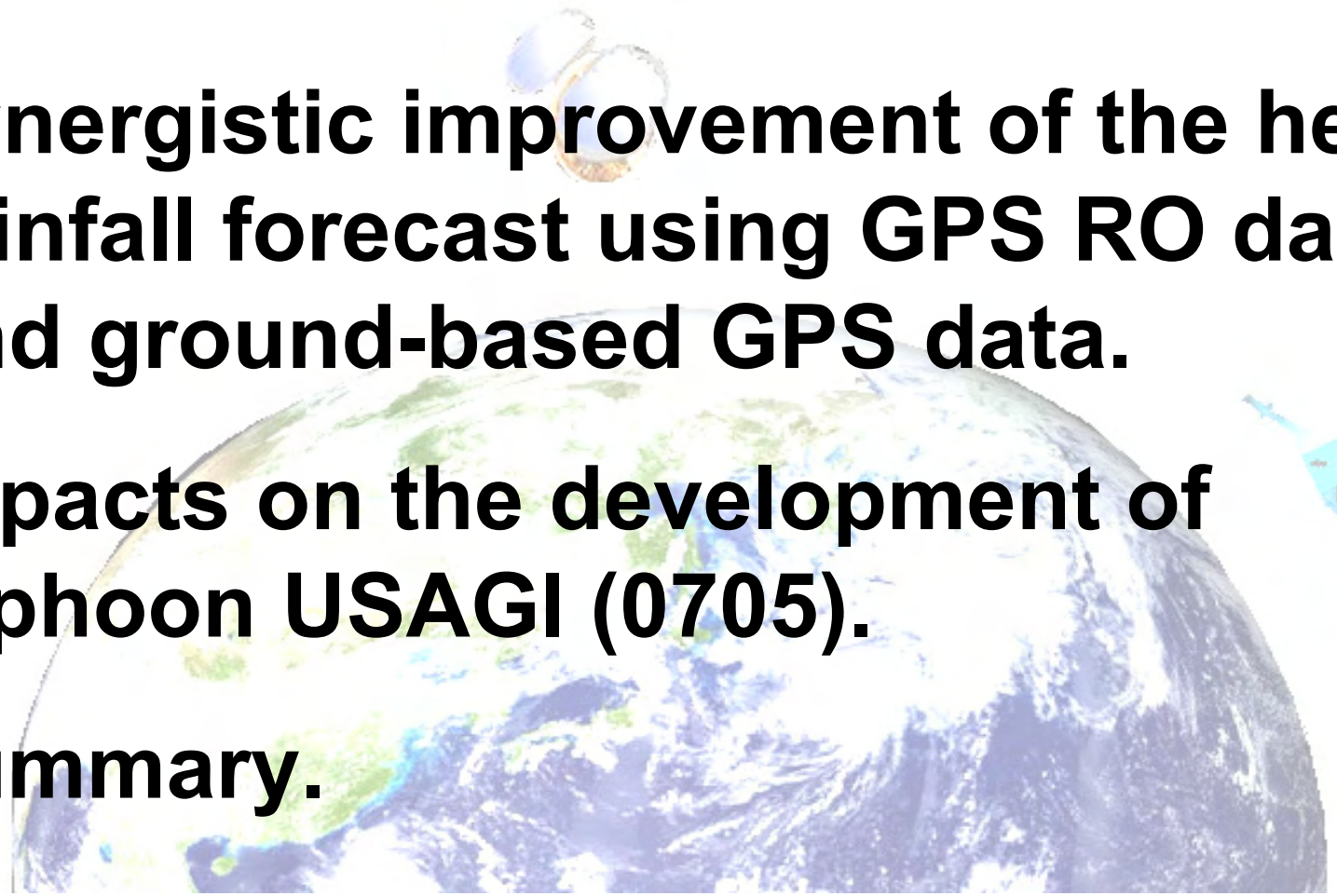

Motivations

- Heavy rainfall often occurs when humid airflow is supplied from the sea.
- Typhoons generated in low latitudes also brought heavy rainfalls.
- Dry air at middle level enhances convections.
- ‘Water vapor distribution over the sea’ and ‘Vertical profile of water vapor’ are important for accurate forecasts.

Motivations

- **‘Water vapor distribution over the sea’ and ‘Vertical profile of water vapor’ are important for accurate forecasts.**
- **GPS radio occultation data is useful data, because it provides these information.**
- **Impacts of GPS radio occultation data on forecasts of heavy rainfall and typhoon are investigated.**

1. Assimilation method of GPS radio occultation data

1a. Torrential rainfall event.

1b. GPS radio occultation data.

1c. Assimilation method.

a. spherical un-uniform distribution
(Tangent point data $\Rightarrow$ Path data)

b. without thinning of data
(Observation error covariance)

Torrential rainfall on 16 July 2004

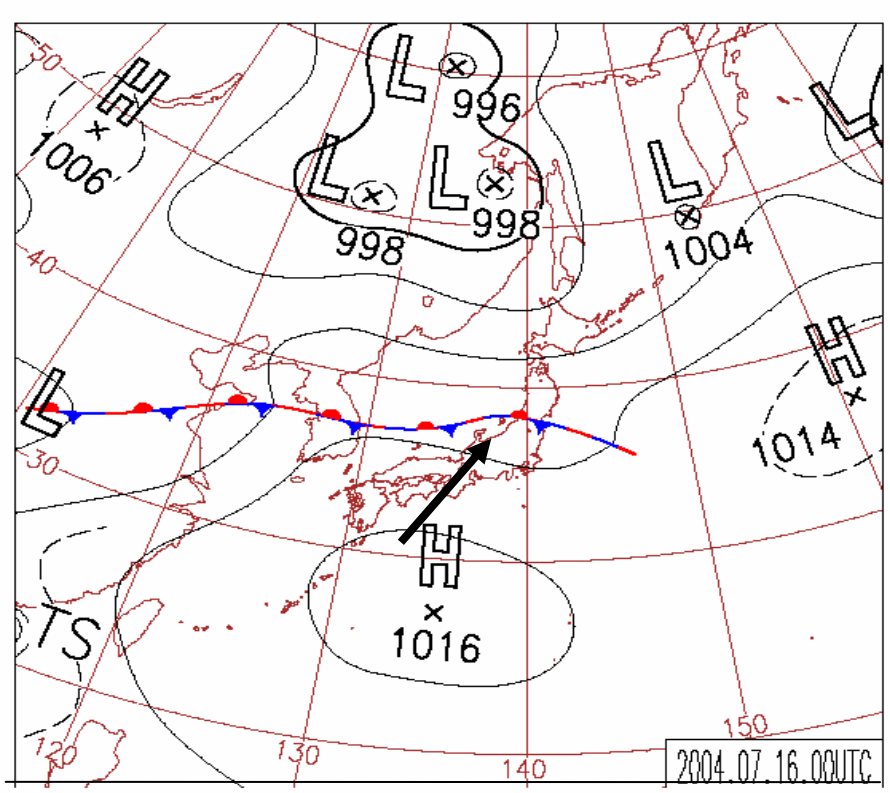

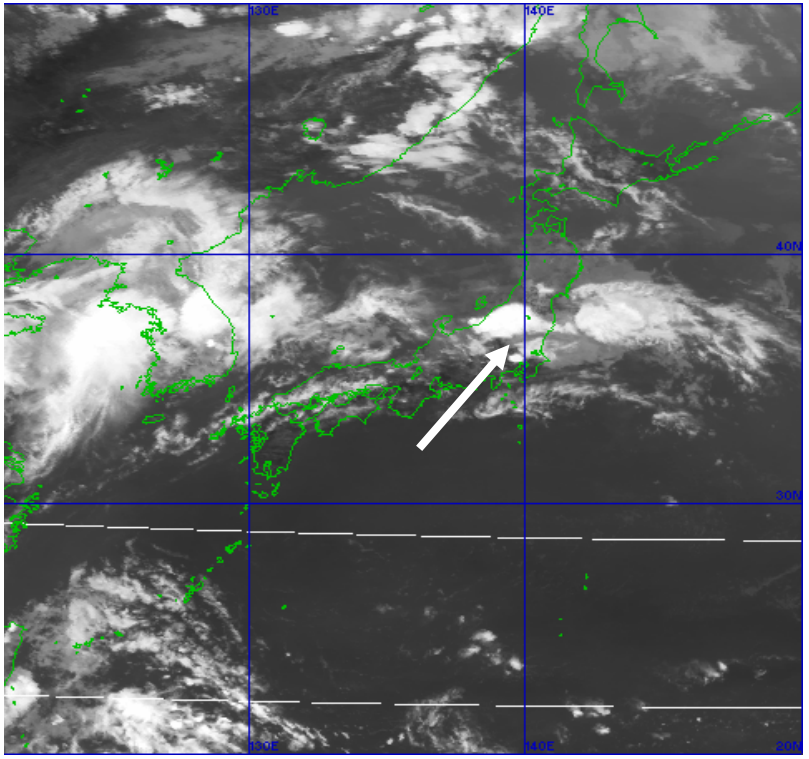

- **Almost every year, heavy rainfalls were caused by Baiu front.**

Torrential rainfall on 16 July 2004

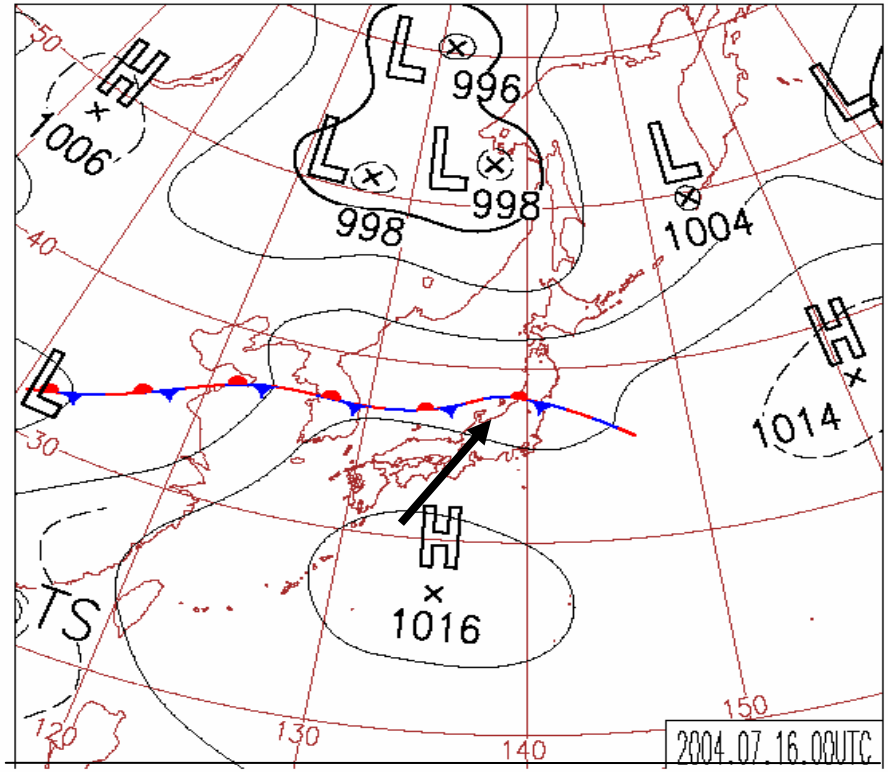

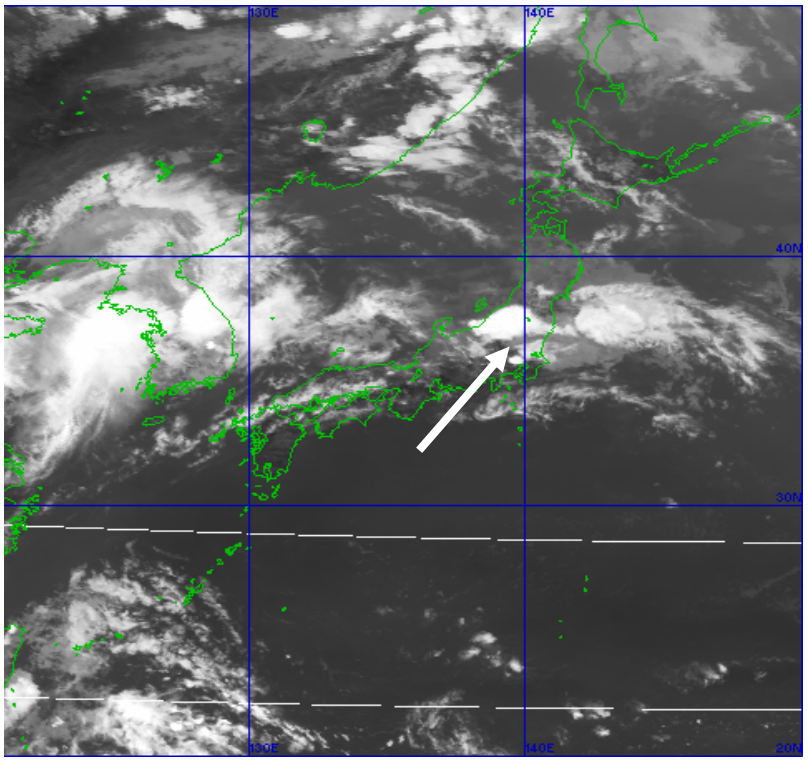

- Baiu front (stationary rainy front) that crossed the northern Japan caused the heavy rainfall.

Torrential rainfall on 16 July 2004

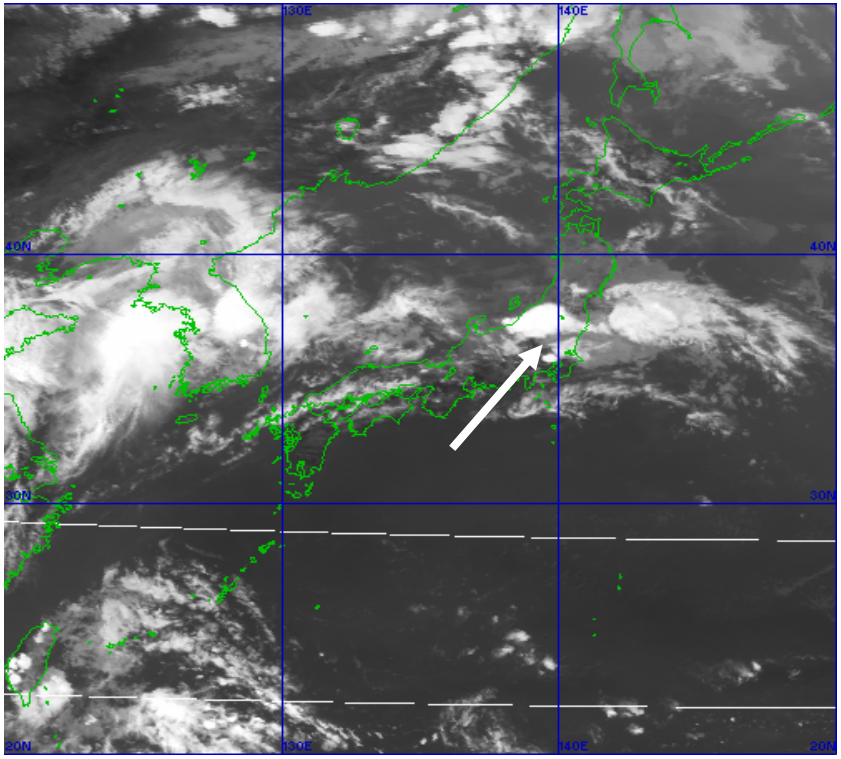

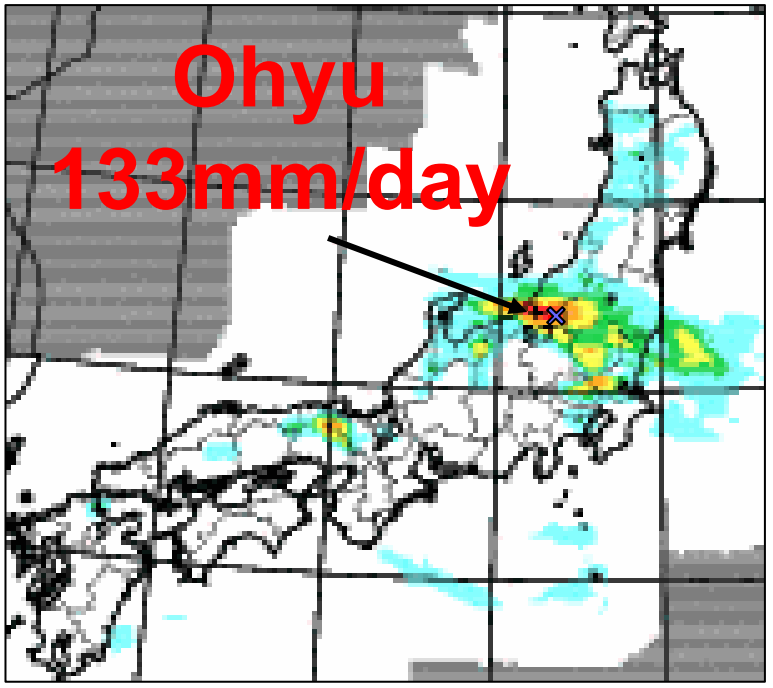

- At Ohyu, rainfall amount of 133mm/day was observed.

GPS radio occultation data

CHAMP/ISDC (GFZ) :

Challenging Mini-Satellite Payload
for Geoscientific Research and Application
Information System and Data Center

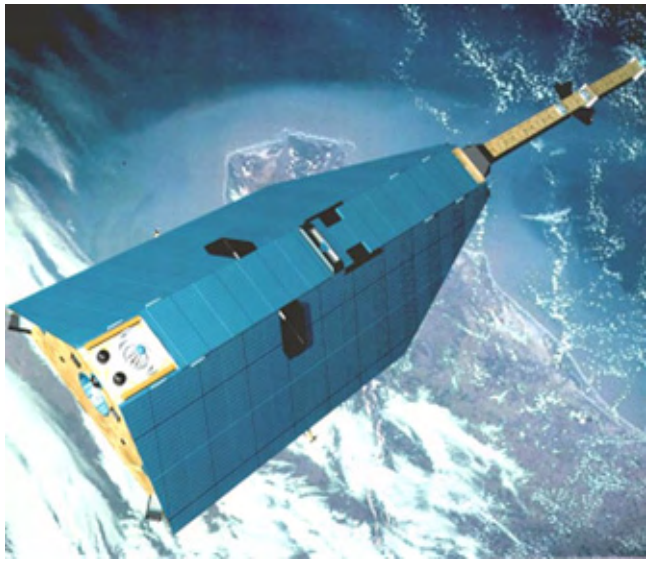

Level 1:Satellite orbit data
Surface reference
Station data

Level 2:Atmospheric phase delay,
Position and moving speed of
CHAMP and GPS satellite.

Level3(1):Profiles of refractive index,
temperature and declination

Level3(2):Profile of water vapor

GPS radio occultation data

CHAMP/ISDC (GFZ) :

Challenging Mini-Satellite Payload
for Geoscientific Research and Application
Information System and Data Center

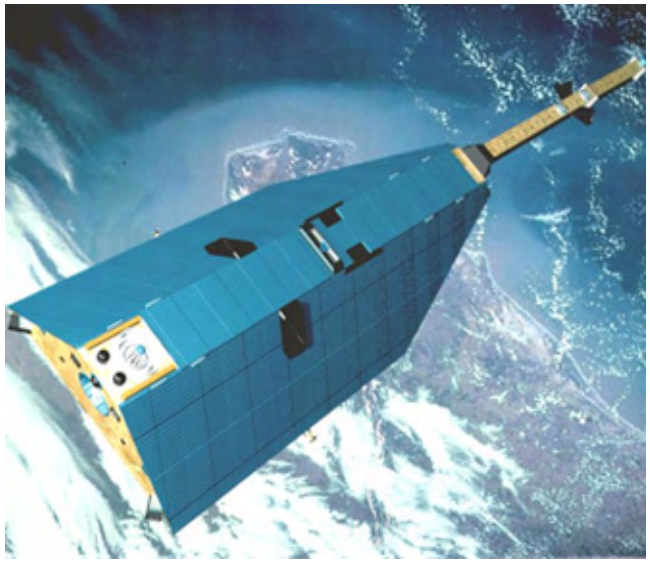

Level3(1):Profiles of refractive index,...

Refractive index(RI):

⇒RI is a function of temperature and water vapor.

$$RI = 1 + 77.6 \times 10^{-6} \frac{P}{T} + 0.373 \frac{e}{T^2}$$

RI is expected to improve rainfall forecasts.

Tangent point data

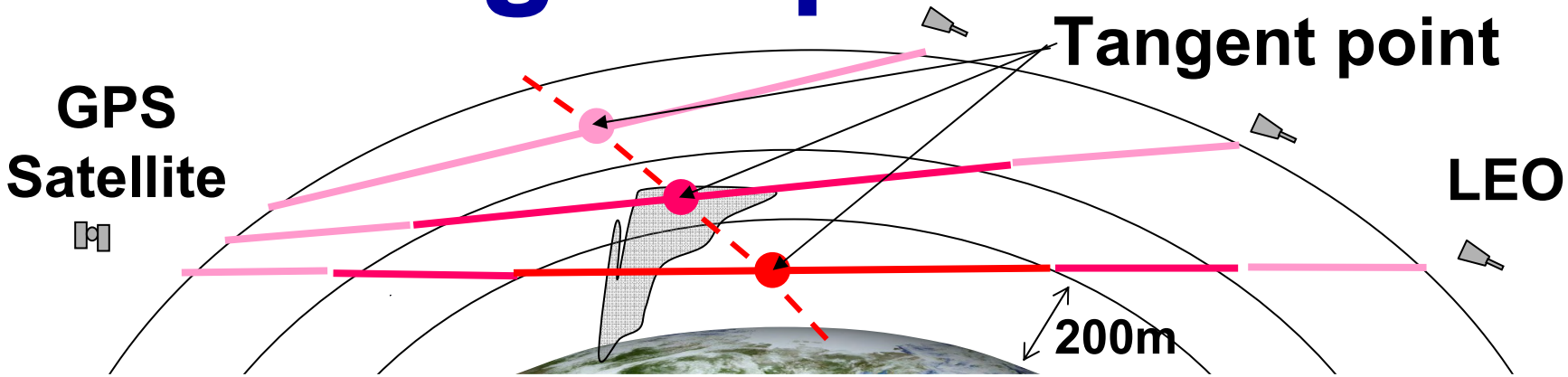

Schematic illustration of estimation of the tangent point data

- Tangent point data was provided.
- Tangent point was the point closest to the earth on the path.
- In the estimation of tangent point data, spherical uniform distribution was assumed.

Assumption of spherical uniform distribution

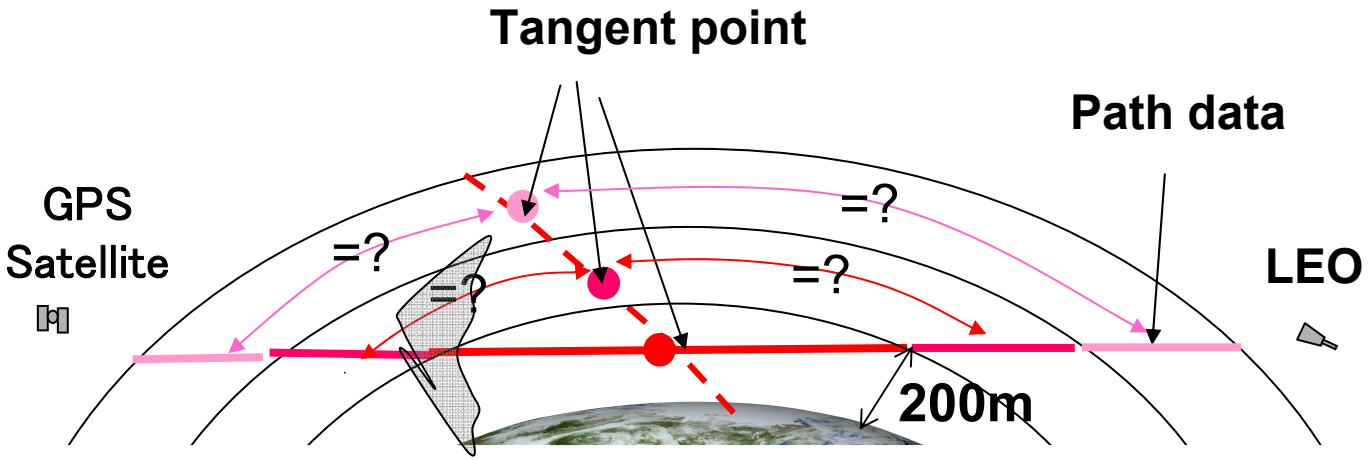

- Using the first guess data of this heavy rainfall case, we investigated the assumption of spherical uniform distribution of RI.

Position of the lowest path

(a) Horizontal position of path data

(b) Vertical position of path data

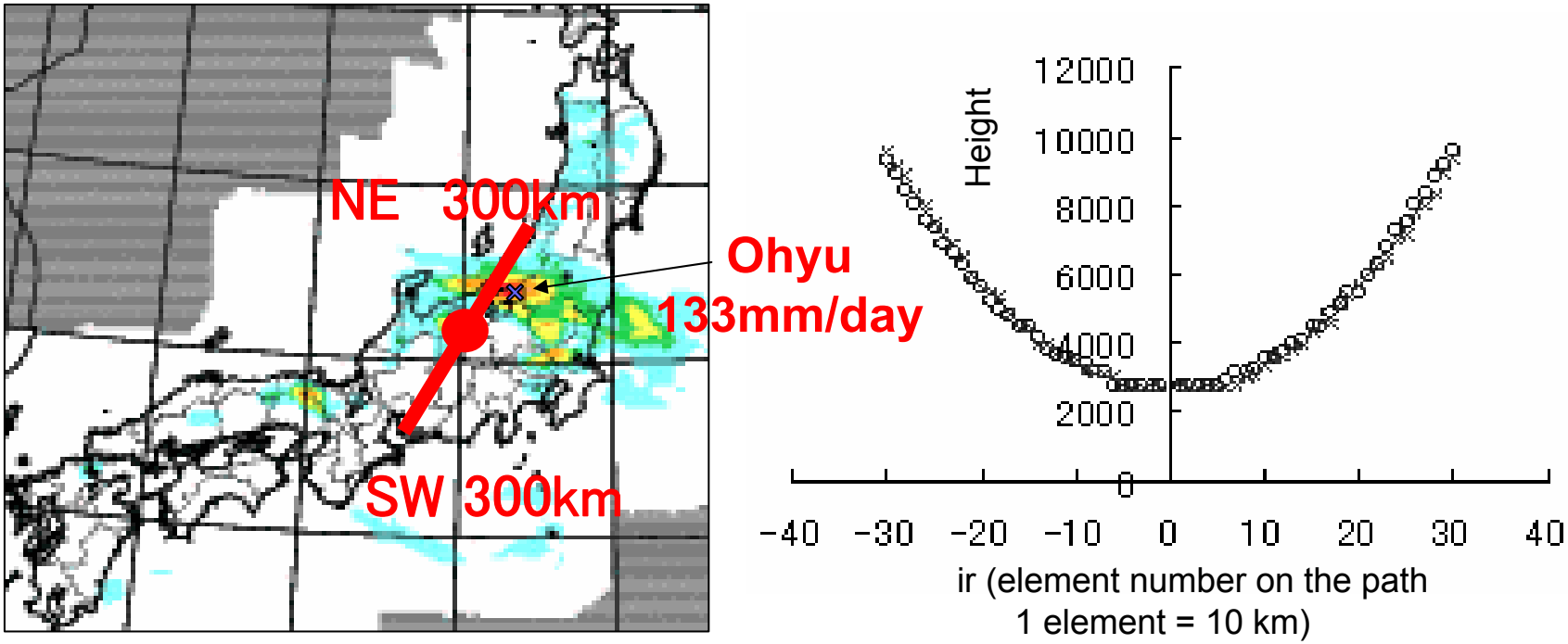

- RO occurred near the rainfall band at 12 JST 16 July, just before the occurrence of heavy rainfall.
- Lowest path penetrated the rainfall band.

Distribution on lowest path

$RI_{path}(z) - RI_{tangentpoint}(z)$

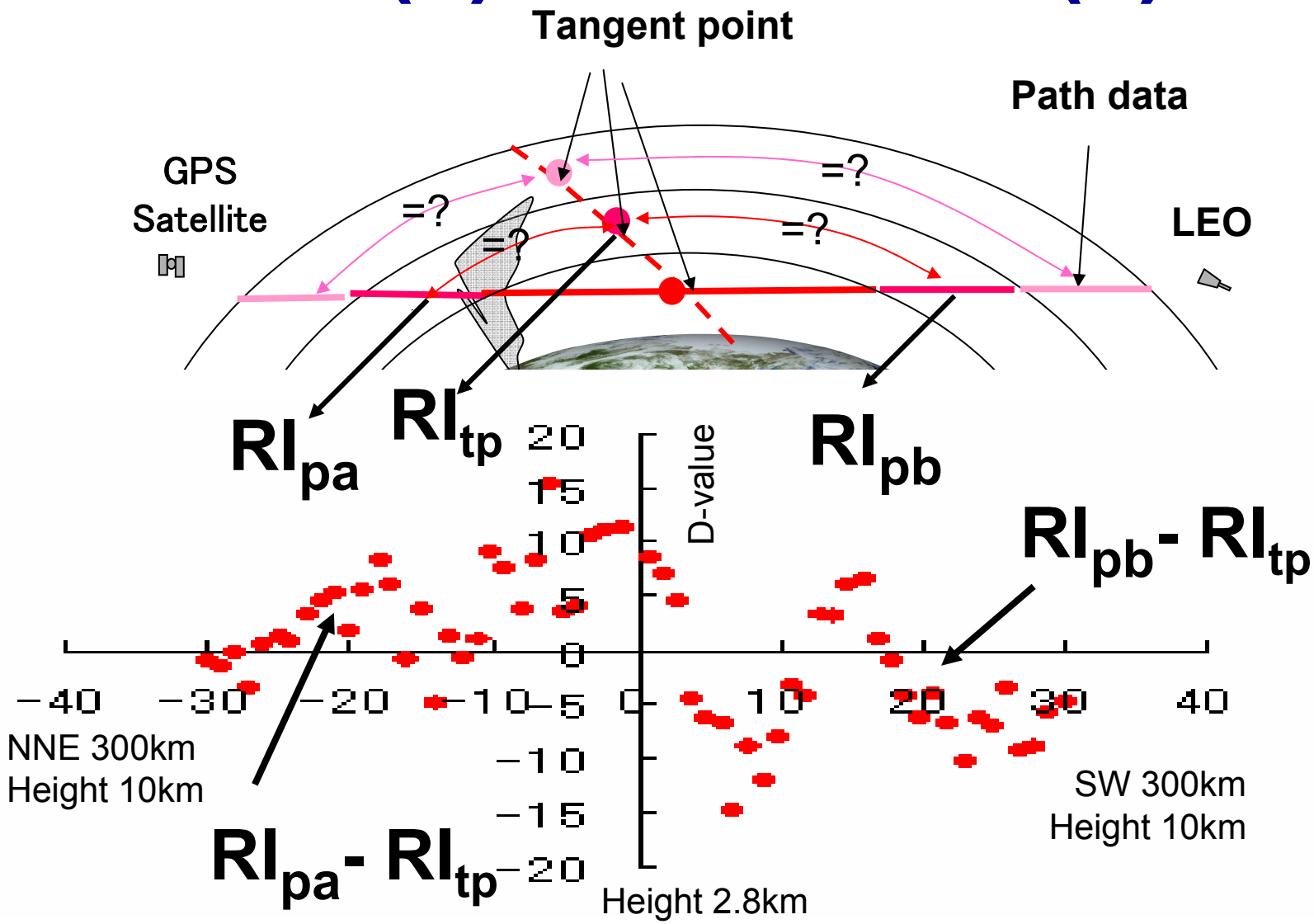

Position of the lowest path

(a) Horizontal position of path data

(b) Vertical position of path data

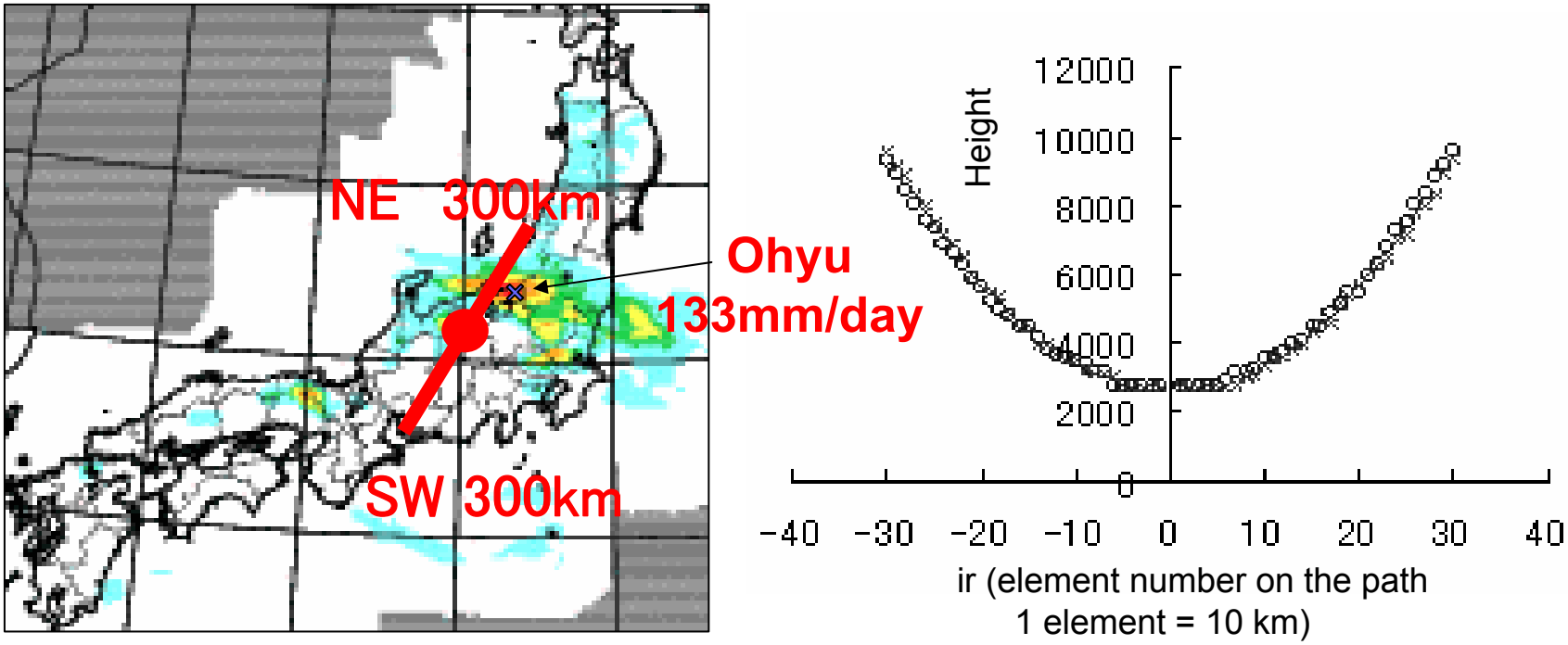

- Was this assumption of spherical uniform distribution was satisfied?

Assumption of spherical uniform distribution

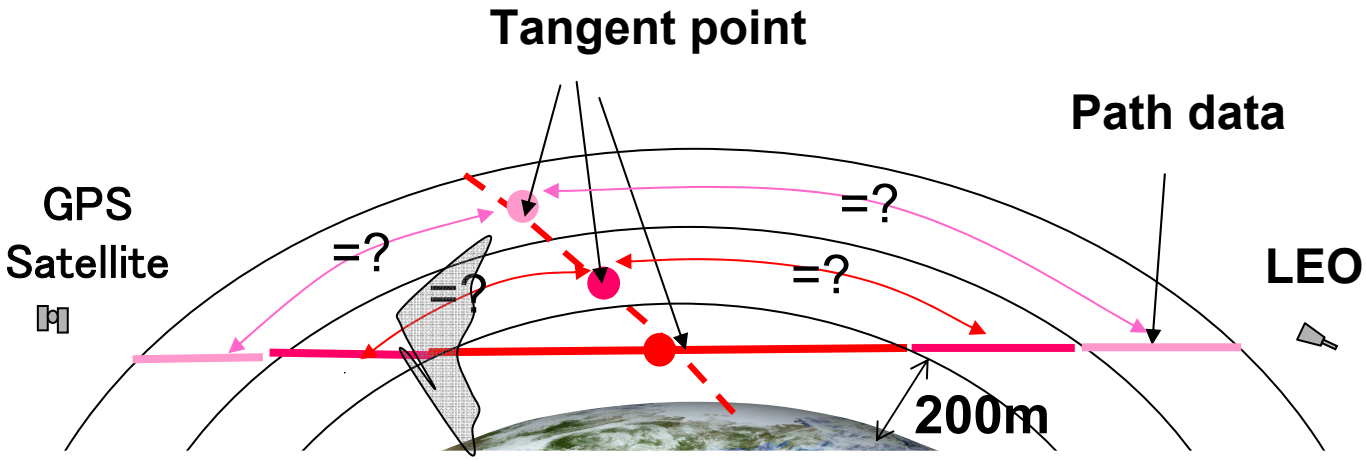

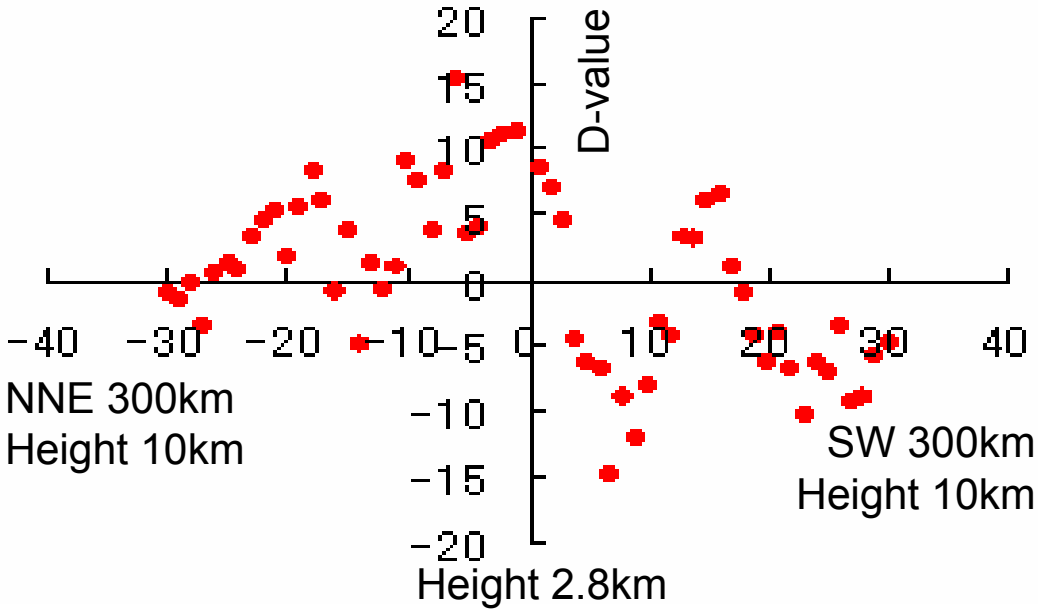

- **Assumption of spherical uniform distribution was not accurate.**

Assumption of spherical uniform distribution

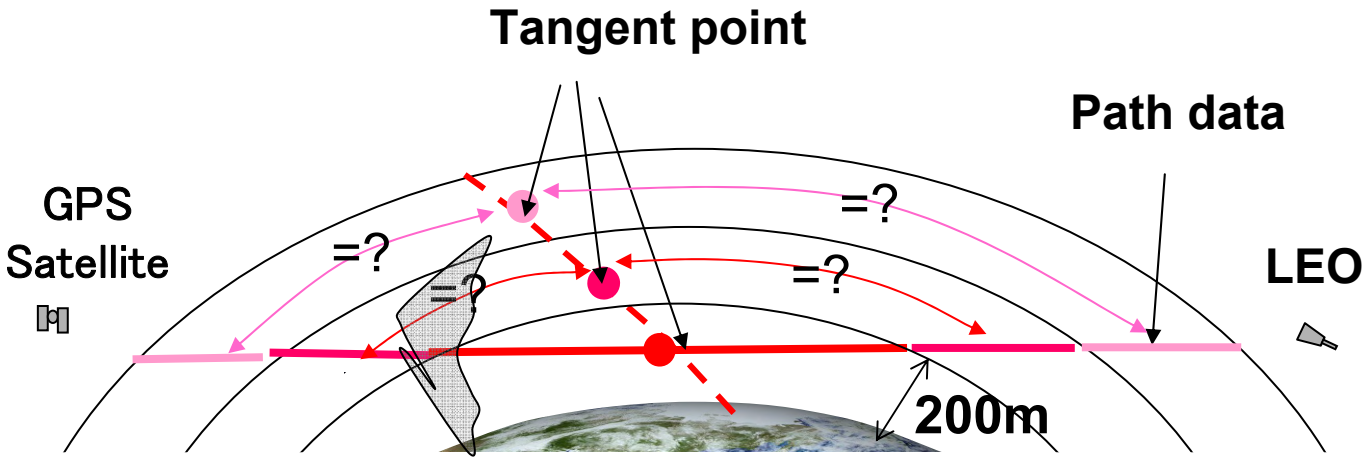

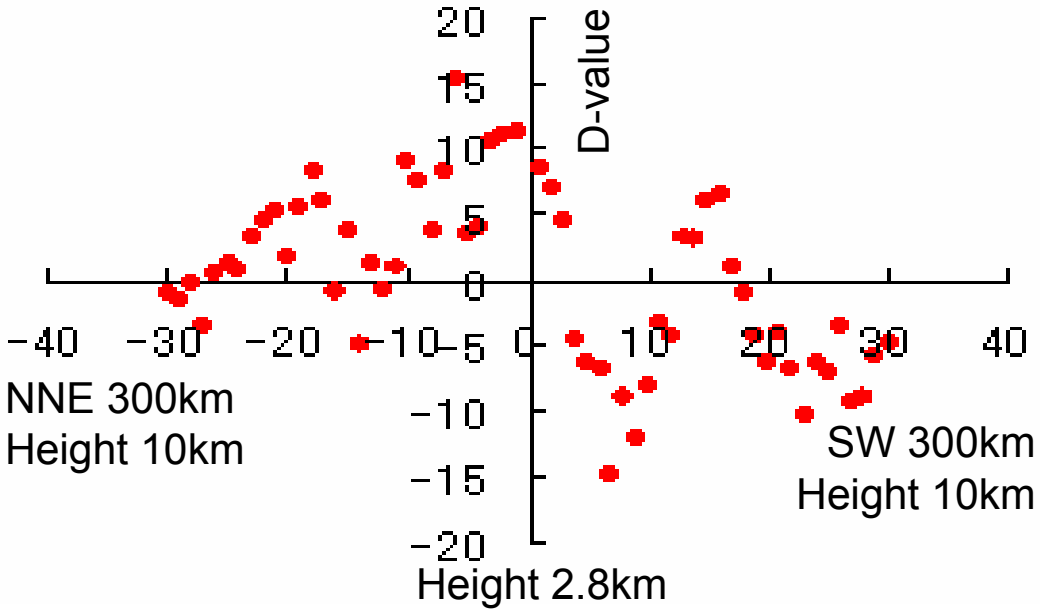

- **Then, we reproduced the path data that does not need to satisfy the assumption.**

Tangent point → Path data

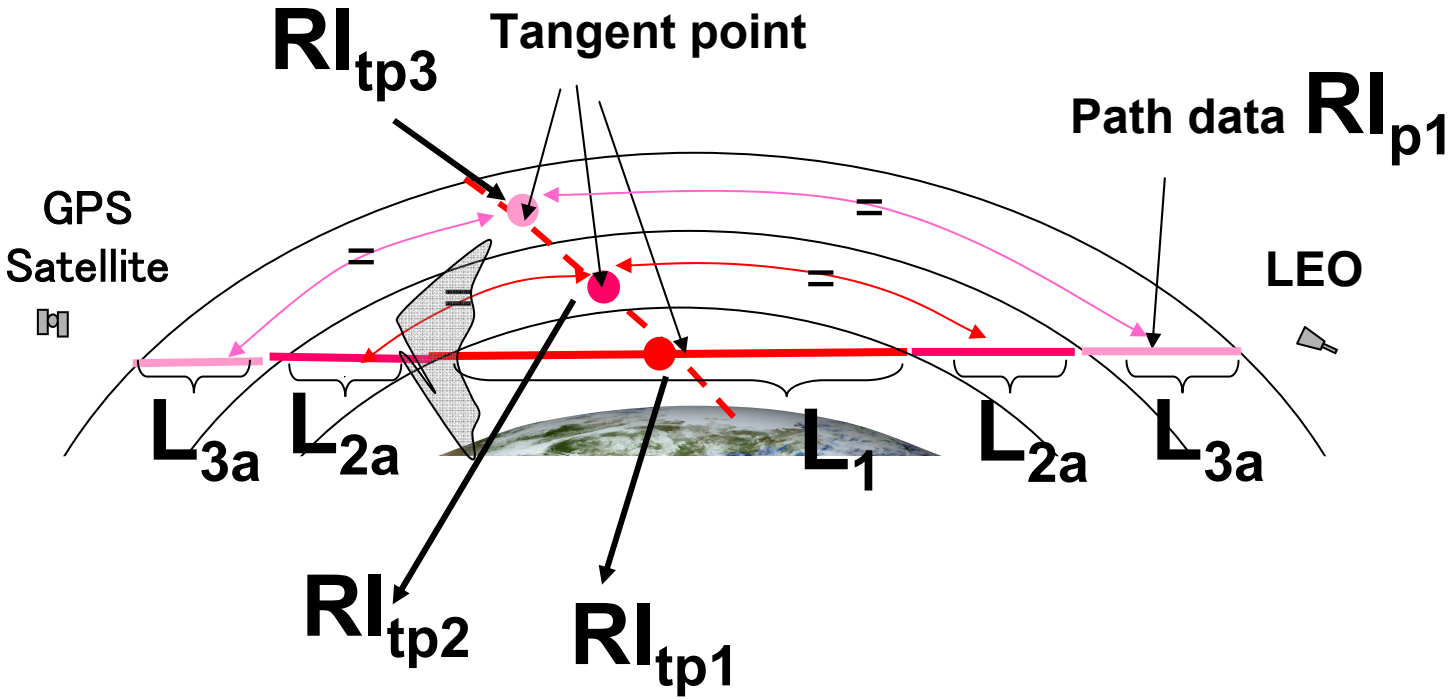

$$RI_{p1} = \frac{L_{3a}RI_{tp3} + L_{2a}RI_{tp2} + L_1RI_{tp1} + L_{2b}RI_{tp2} + L_{3b}RI_{tp3}}{L_{3a} + L_{2a} + L_1 + L_{2b} + L_{3b}}$$

- **Path data was reproduced from tangent point data by path-length weighting average.**

First guess of Path data

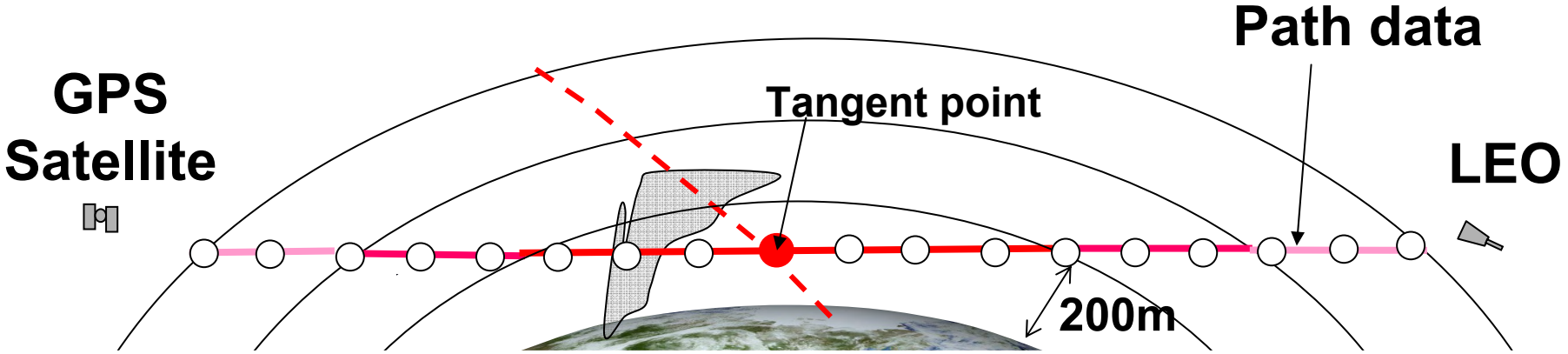

$$RI_{first\_guess\_of\_path} = \frac{\sum_{i=1}^{n(height<10km)} RI_{first\_guess\_of\_point}}{n}$$

-*n* is the total number of elements under the height of 10km.

- **First guess was produced by averaging RI on the path.**

Observed and first guess profiles of the path data

- Observed RI was **larger than that of first guess below 5 km.**
- The rainfalls is expected to be intensified by the assimilation of RO data.

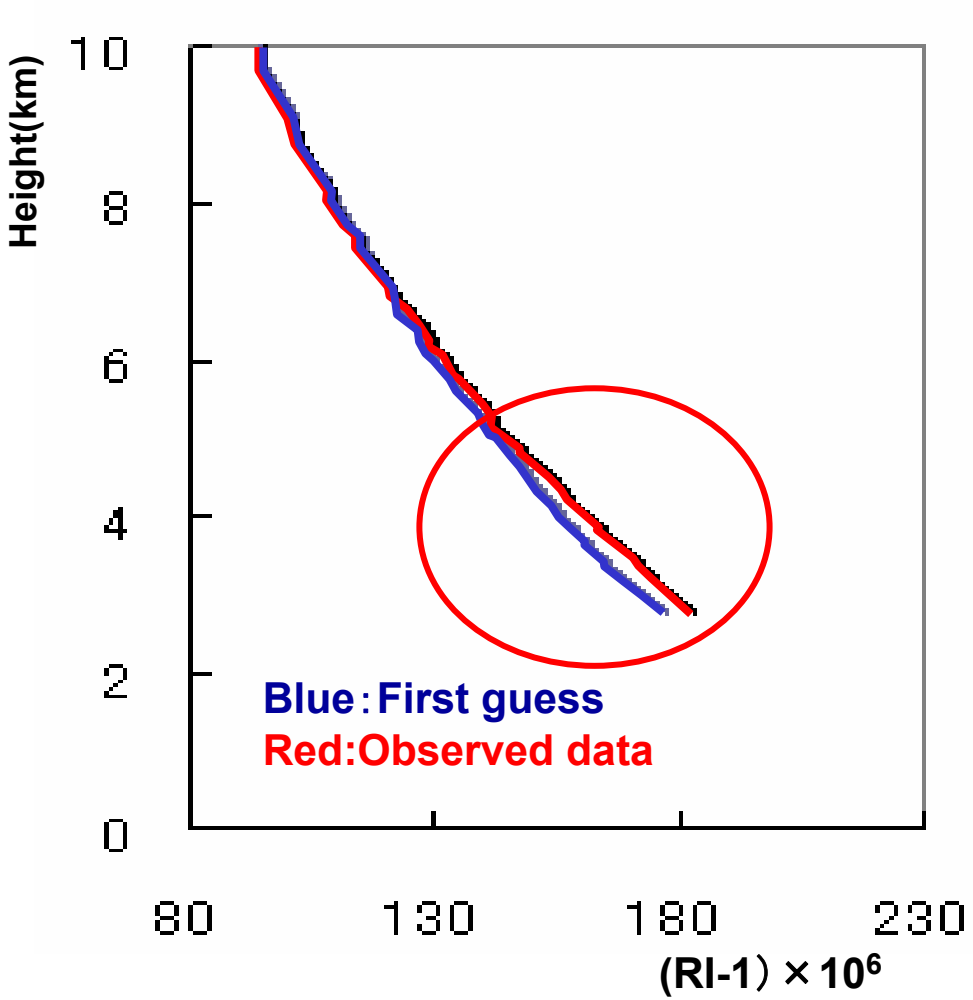

Correlation of Observation Error

- **Observation error has vertical correlation.**
  (vertical resolution, path data)
- **In general, thinning of the data is performed. However, thinning might remove the informative data.**
- **Observation error covariance was produced and used in the assimilation.**

Correlation of Observation Error

- **Vertical correlation was considered by following Chen et al (2005).**

(1) D-value of each height:

$$x_i = DN^i_{obs\_err} = DN^i_{obs(t)-mdl(t)} - \frac{t}{12} DN^i_{mdl(t')-mdl(t'-12)} \qquad (1)$$

NMC method

(2) Correlation of Obs. Err.:

$$r_{k_1 k_2} = \frac{\overline{x_{k_1} x_{k_2}} - \overline{x_{k_1}}\,\overline{x_{k_2}}}{\sqrt{\overline{x_{k_1}^2} - \left(\overline{x_{k_1}}\right)^2}\sqrt{\overline{x_{k_2}^2} - \left(\overline{x_{k_2}}\right)^2}} \qquad (2)$$

Correlation of Observation Error

(3) Observation covariance:

$$\mathbf{R} = \begin{pmatrix} r_{11}\sigma_1^{\,2} & r_{21}\sigma_1\sigma_2 & \cdots & r_{n1}\sigma_1\sigma_n \\ r_{12}\sigma_1\sigma_2 & r_{22}\sigma_2^{\,2} & \cdots & \vdots \\ \vdots & \vdots & \ddots & \vdots \\ r_{1n}\sigma_1\sigma_n & \cdots & \cdots & r_{nn}\sigma_n^{\,2} \end{pmatrix} \qquad (3)$$

Obs. Err. of each height

(a) Correlation of obs.err.(r_{ij})

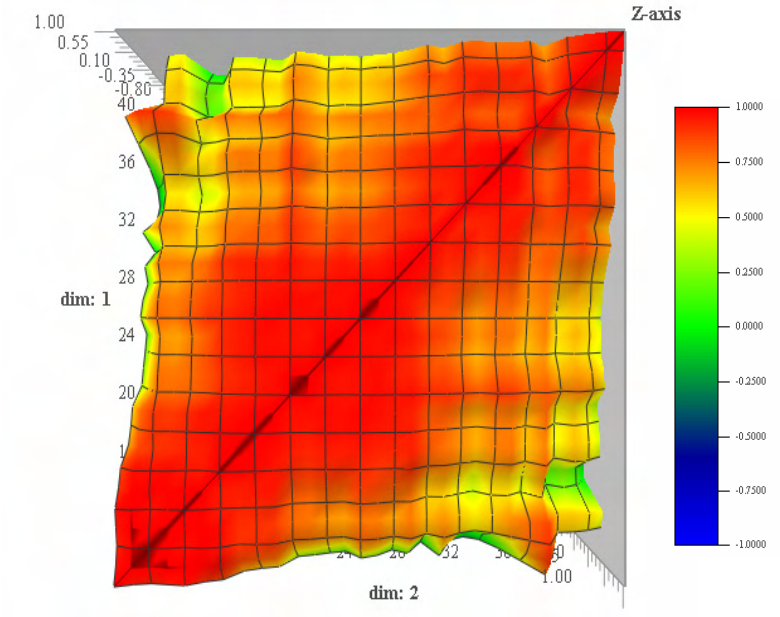

(b) Simplified obs. covariance (R)

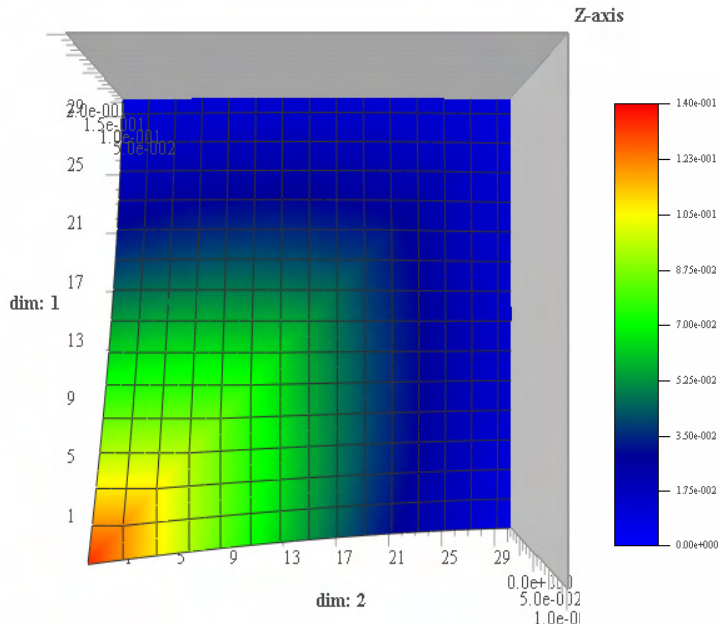

2. Synergistic improvement using GPS RO data and ground-based GPS data

2a. Assimilation method of ground-based GPS data.

2b. Impact of GPS RO data and ground-GPS data.

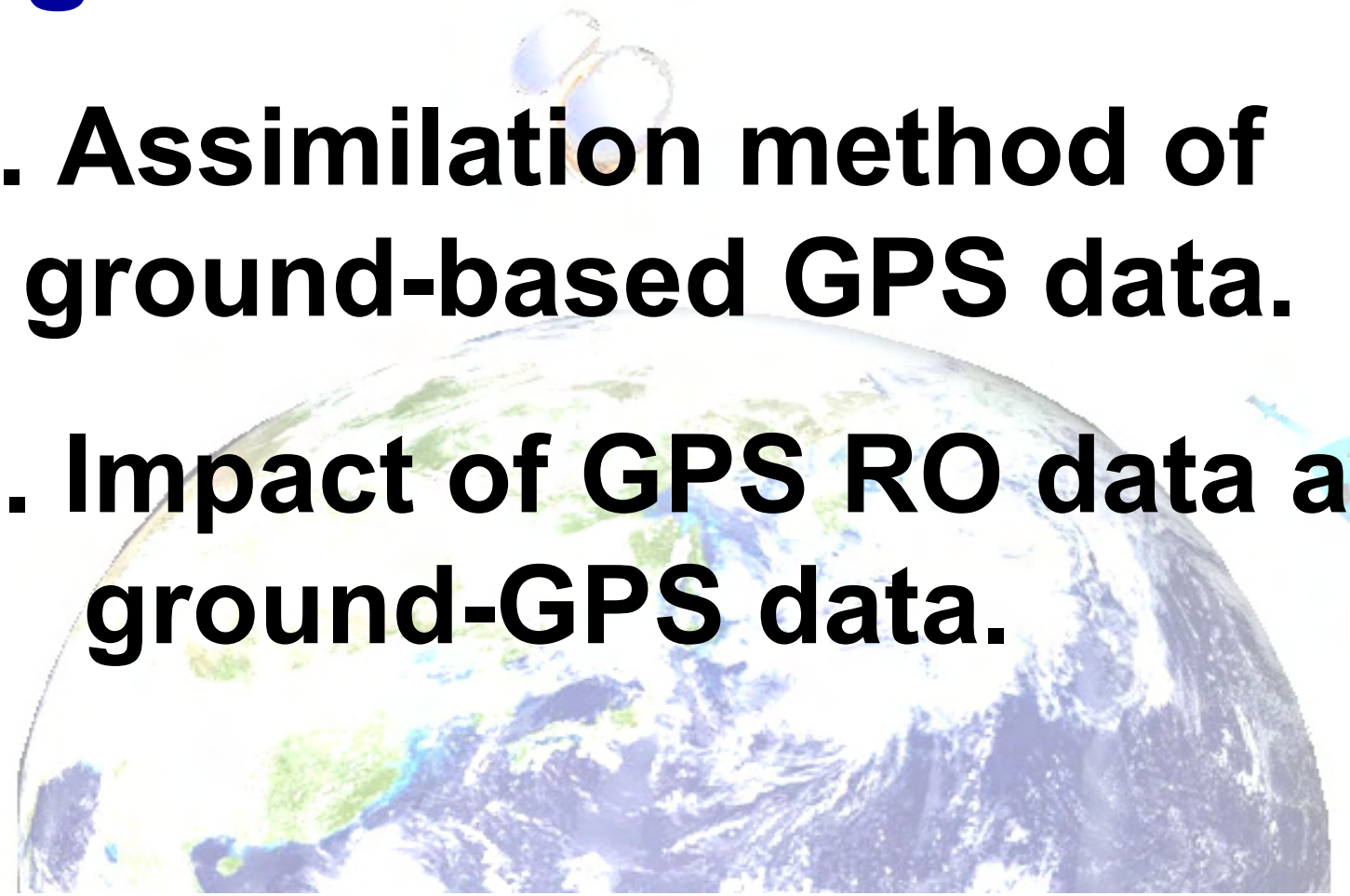

Ground-based GPS data
- Estimation of Zenith Total Delay-

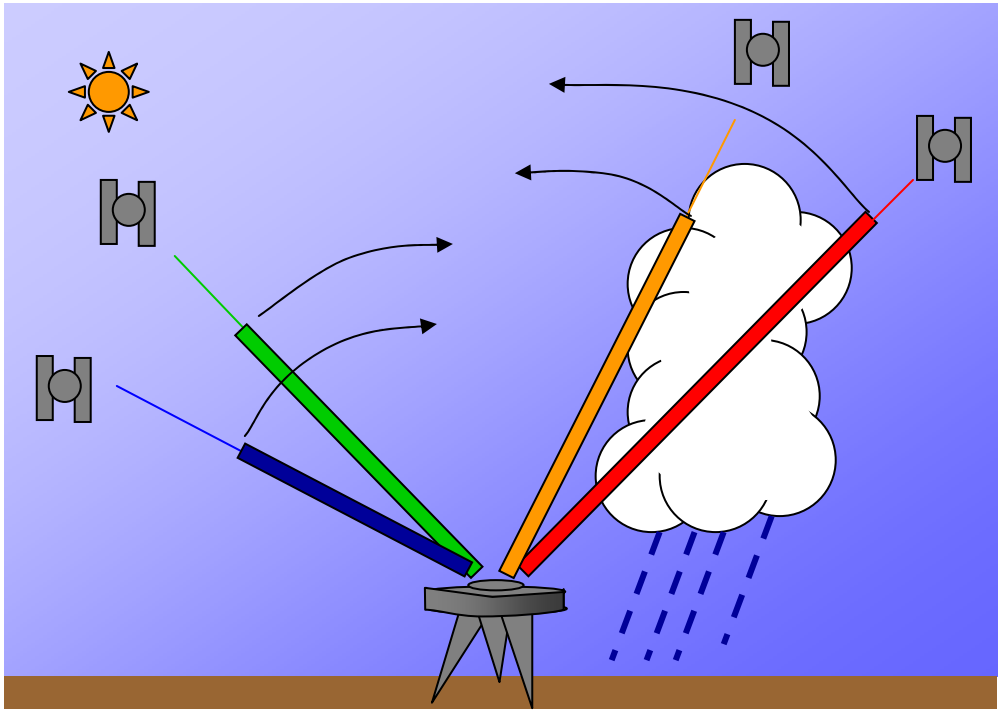

- **Zenith Total Delay (ZTD) was obtained by GPS software (GIPSY) .**

1. **Slant total delay was converted to value of zenith direction.**

Ground-based GPS data
- Estimation of Zenith Total Delay-

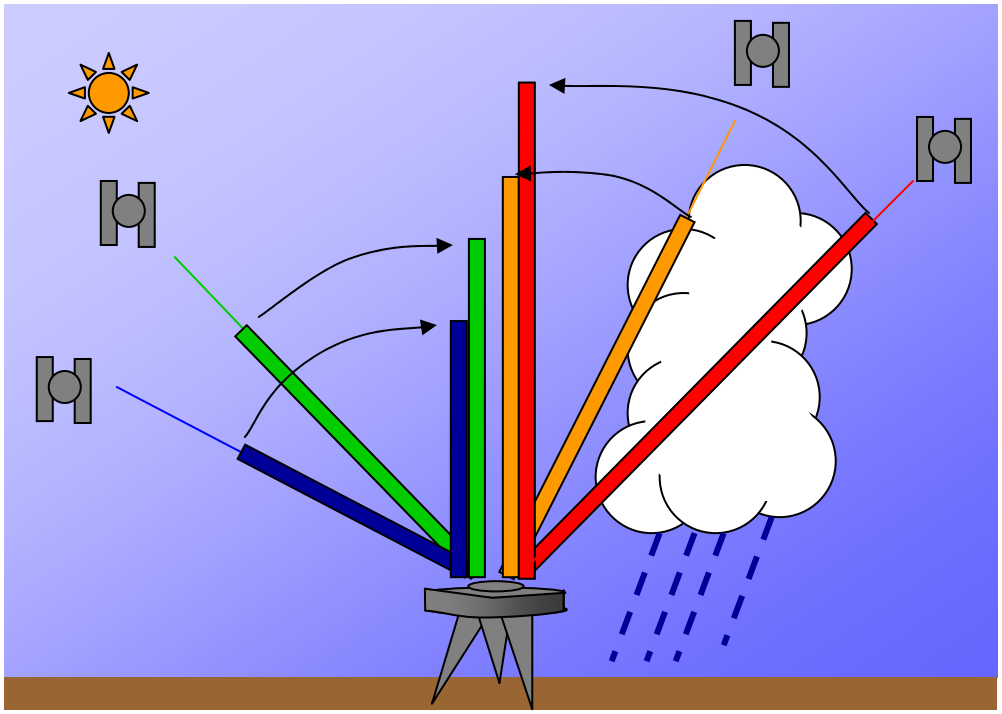

- **Zenith Total Delay (ZTD) was obtained by GPS software (GIPSY) .**

1. **Slant total delay was converted to value of zenith direction.**

Ground-based GPS data
- Estimation of Zenith Total Delay-

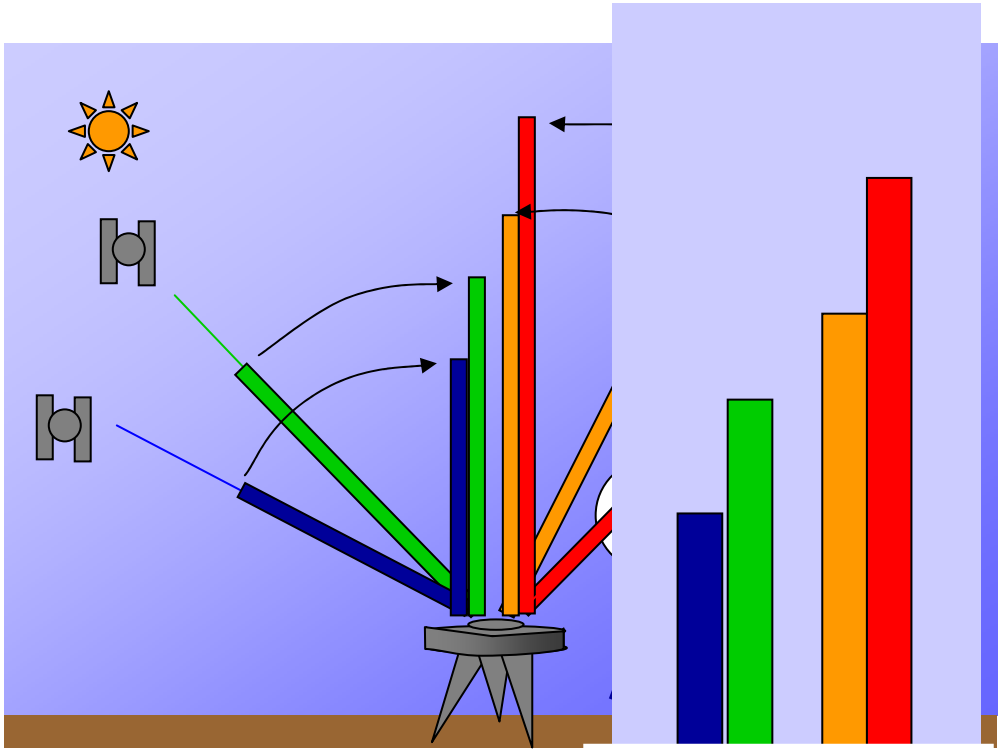

- **Zenith Total Delay (ZTD) was obtained by GPS software (GIPSY) .**

2. By applying the mapping factor, which is model of delay distribution, ZTD was estimated.

Ground-based GPS data
- Estimation of Zenith Total Delay-

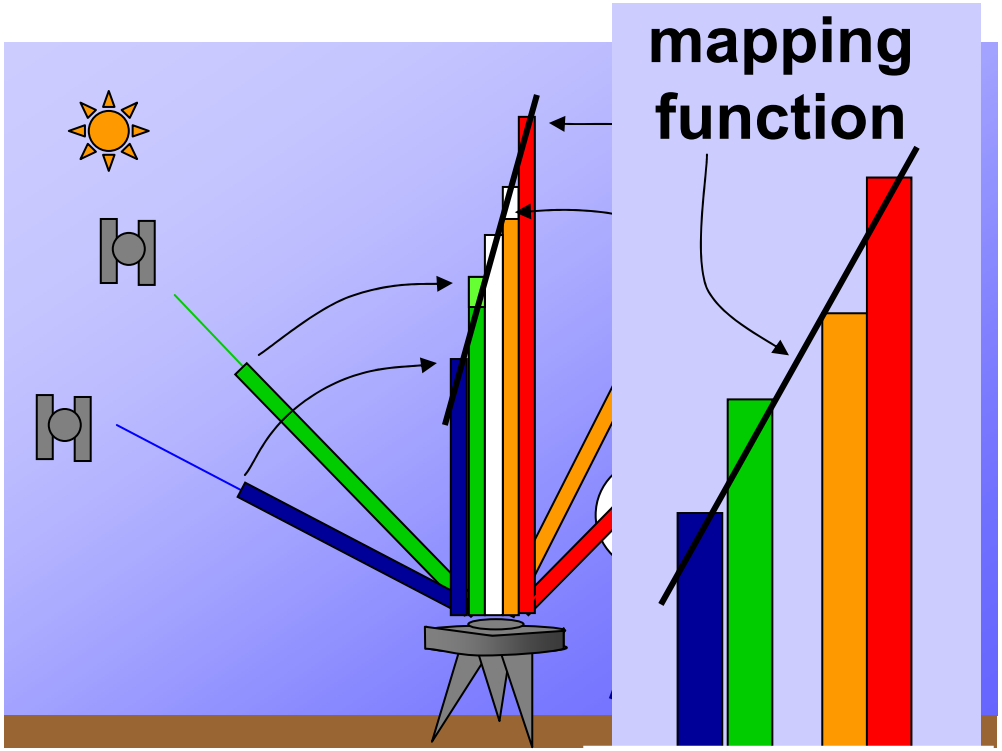

- Zenith Total Delay (ZTD) was obtained by GPS software (GIPSY) .

2. By applying the mapping factor, which is model of delay distribution, ZTD was estimated.

Ground-based GPS data
- Estimation of Zenith Total Delay-

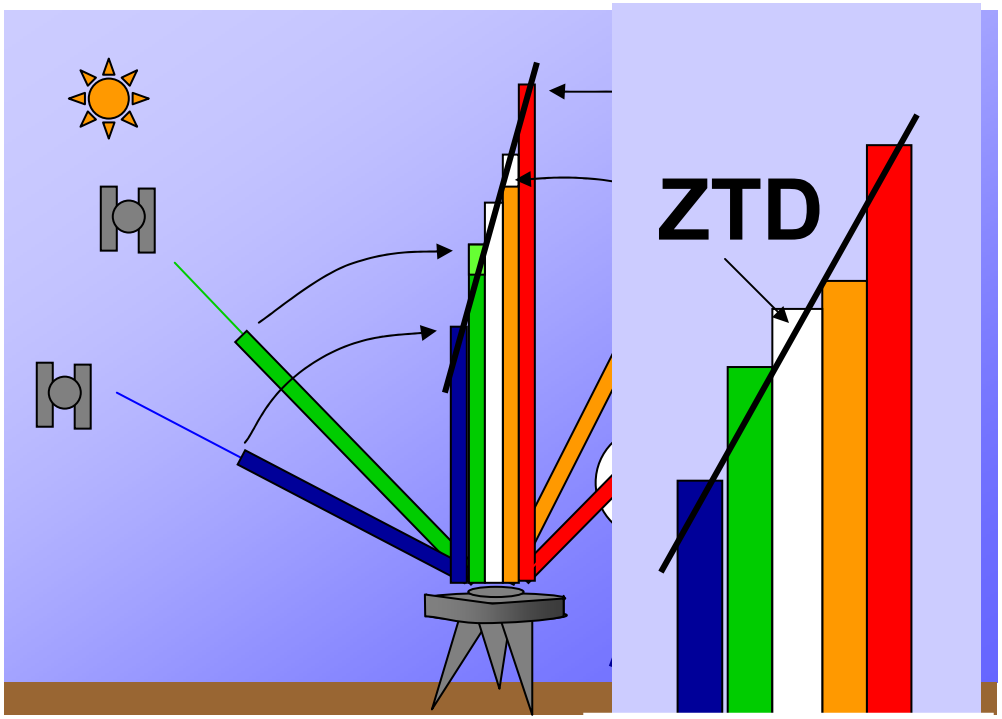

- Zenith Total Delay (ZTD) was obtained by GPS software (GIPSY) .

2. By applying the mapping factor, which is model of delay distribution, ZTD was estimated.

Ground-based GPS data
- Estimation of Zenith Total Delay-

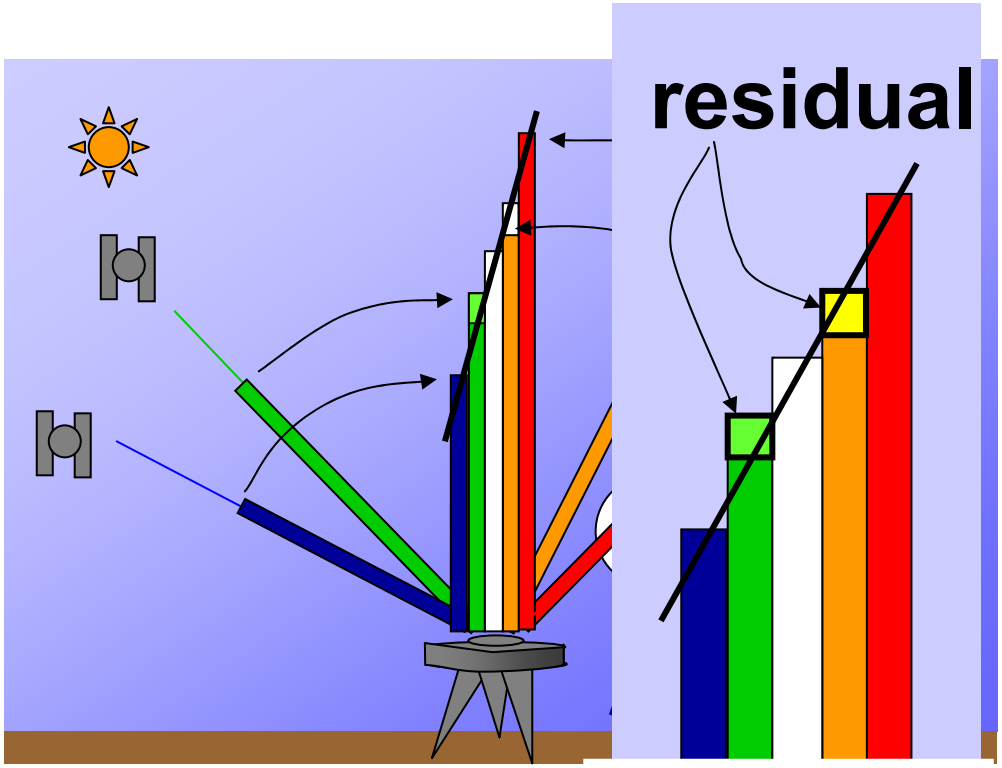

- Zenith Total Delay (ZTD) was obtained by GPS software (GIPSY) .

3. Residuals, the differences of STD from the modeled delay, are also obtained.

Ground-based GPS data
- Estimation of Slant Total Delay-

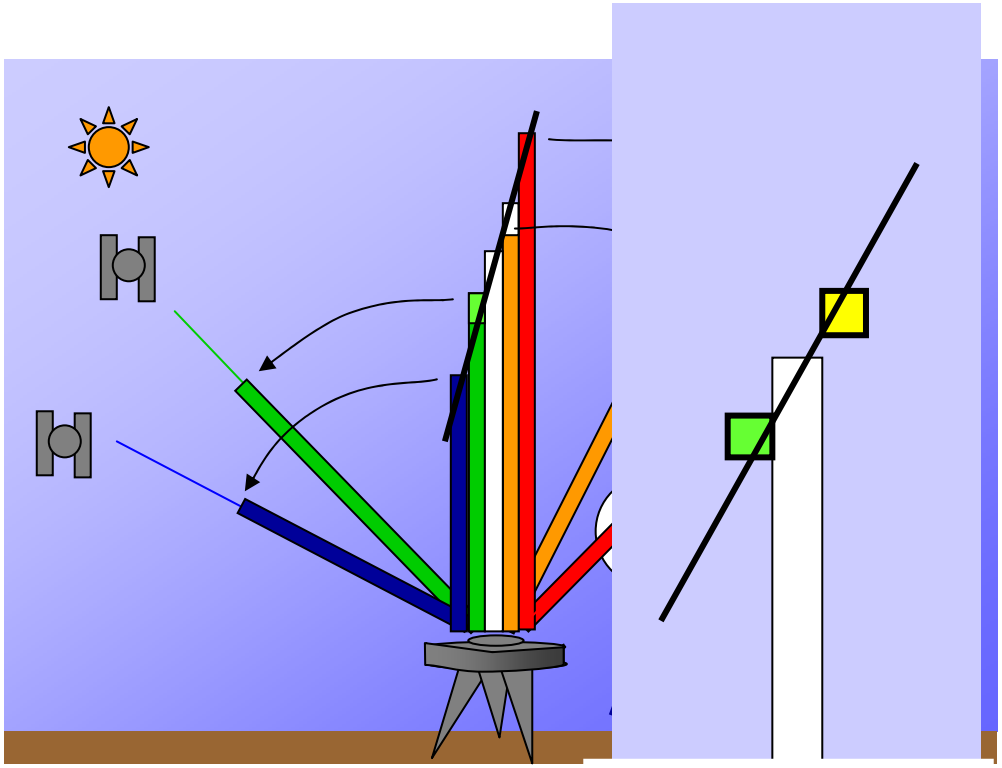

- **Slant total delay (STD) is estimated from ZTD, mapping function etc.**

4.We retrieved STD from ZTD, mapping function and residuals.

Ground-based GPS data
- Estimation of Slant Total Delay-

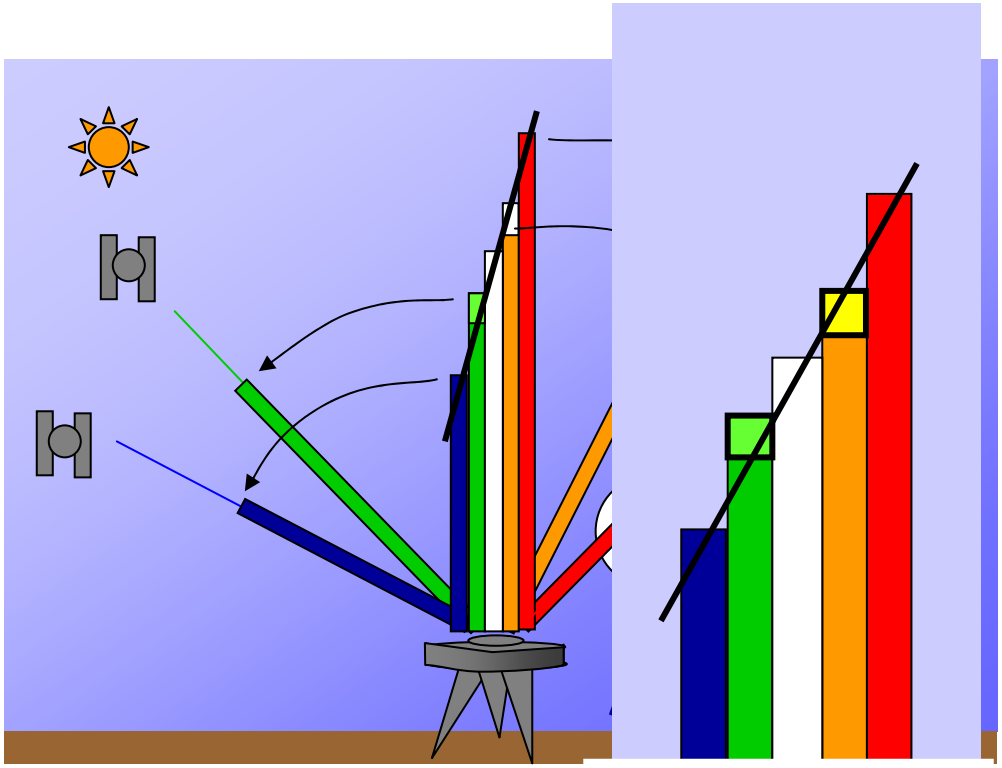

- **Slant total delay (STD) is estimated from ZTD, mapping function etc.**

4.We retrieved STD from ZTD, mapping function and residuals.

ZTD,STD → PWV,SWV

- **PWV is estimated using surface pressure and temperature.**

$$ZTD = ZHD + ZWD$$

$$ZHD = 10^{-6}\frac{R}{m_d}g_m P_{sfc}$$

$$g_m = \frac{\int \rho(z) g(z) dz}{\int \rho(z) dz}$$

$$ZWD = \Pi^{-1} \times PWV$$

$$\Pi = \frac{10^5}{R}\left(k_2 - k_1\frac{m_v}{m_d} + \frac{k_1}{T_m}\right)$$

$$T_m = \frac{\int \frac{P_v}{T} dz}{\int \frac{P_v}{T^2} dz}$$

$$T_m \approx 70.2 + 0.72 T_{sfc}$$

- **SWV is estimated using the same procedures from STD.**

Paths of RO and ground-GPS data

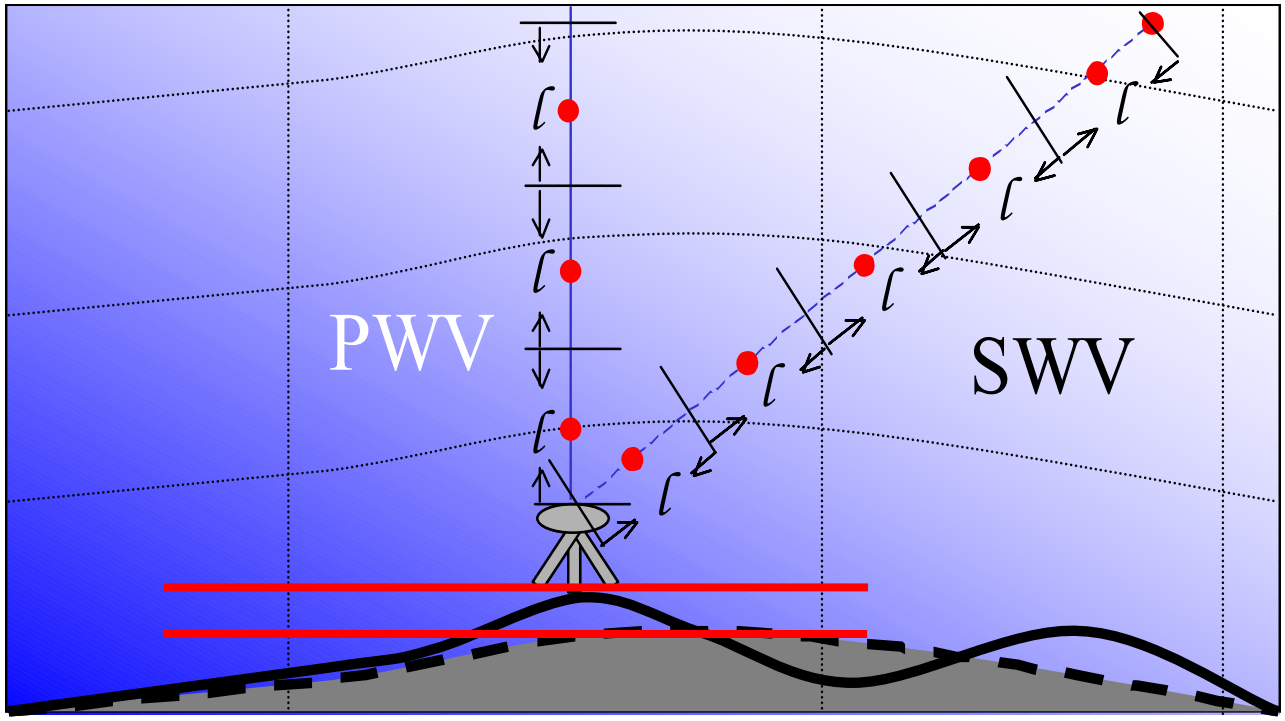

- First guess was produced by integrating of water vapor along the path.
- Influence of difference of altitudes was corrected by the observed surface pressure and temperature.

Positions of RO and ground-based GPS data

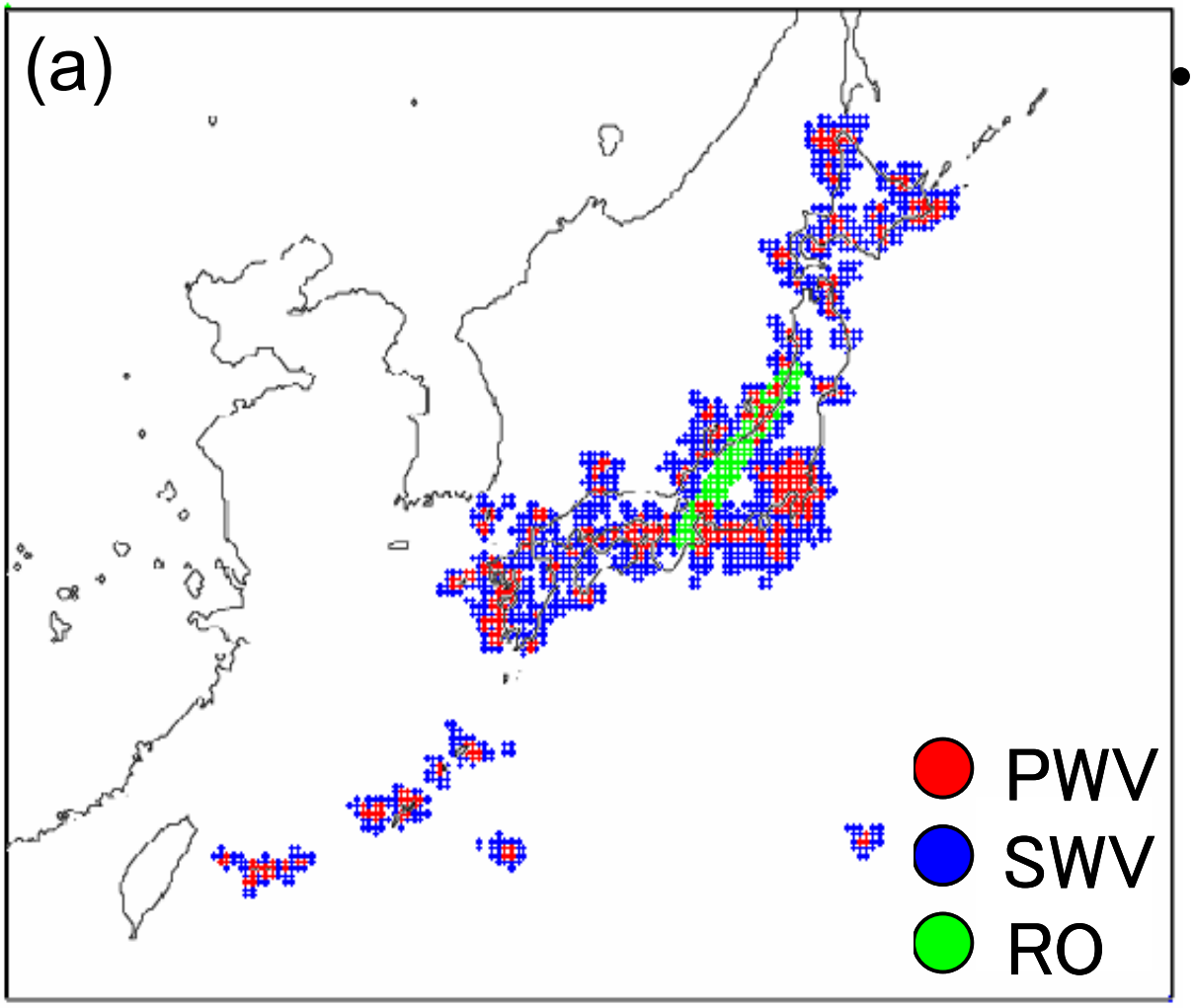

- Grid distribution of which spatial interpolation weights ere positive in the assimilations of ground-based GPS data (PWV, SWV) and RO data.

D-values of ground-based GPS data

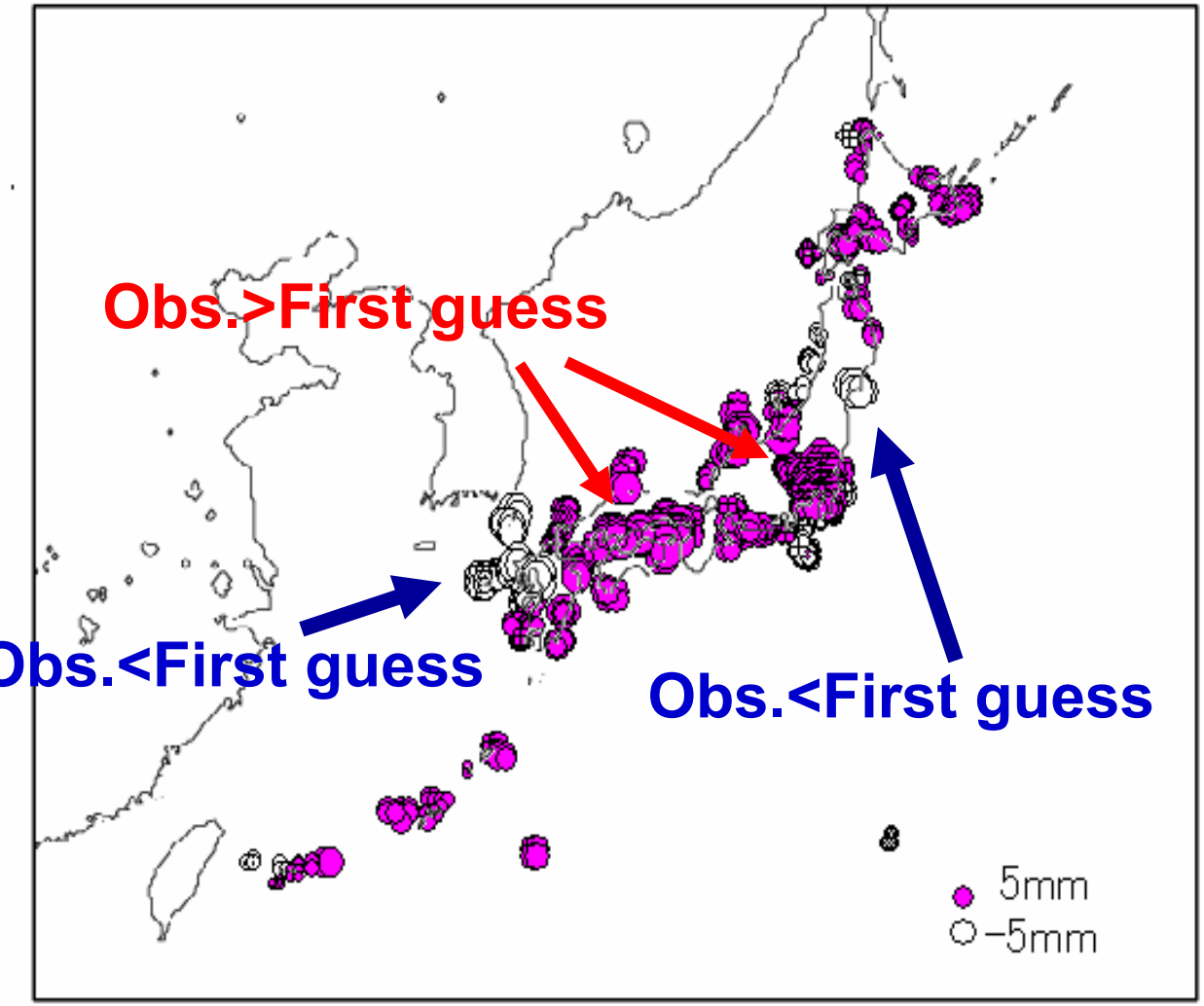

- D-value of PWV (Obs.-First guess) from 12 JST to 15 JST.

Rainfalls region predicted from analyzed fields (conventional data)

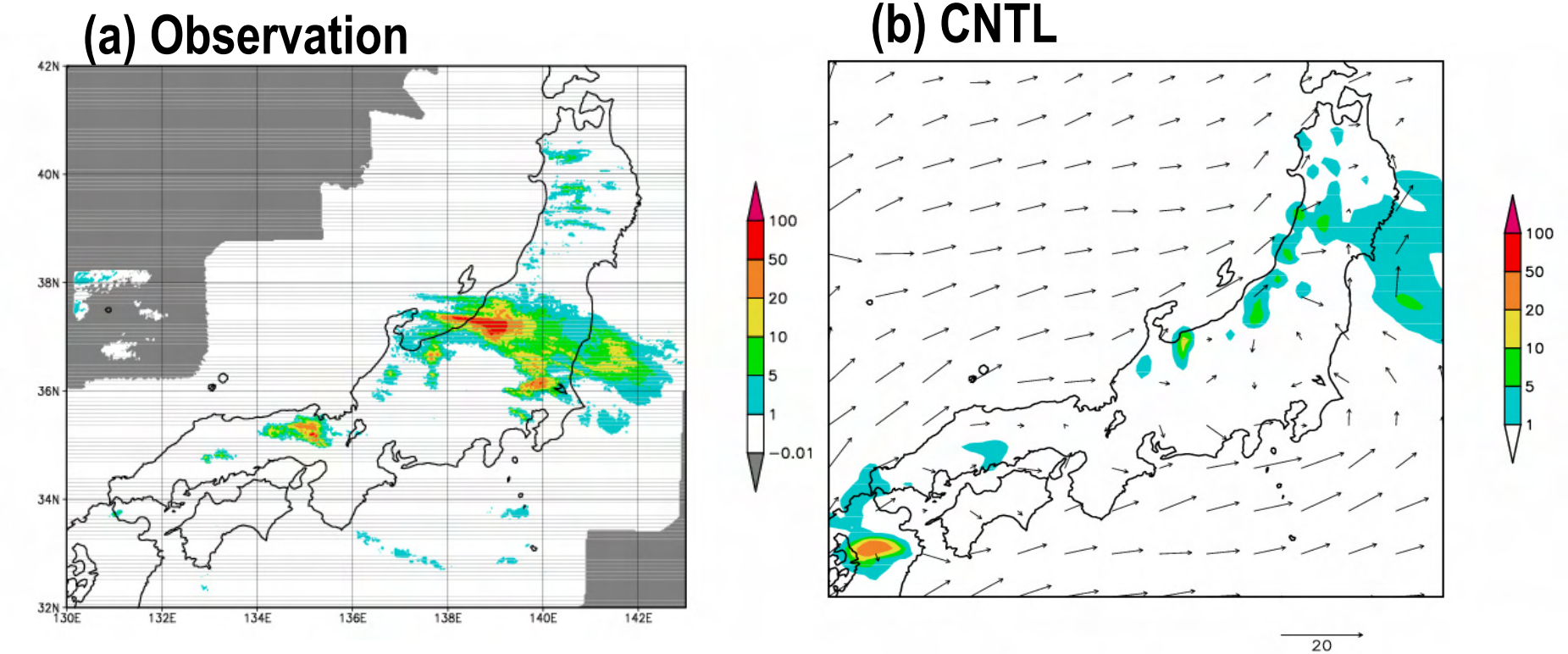

Three hour rainfall of forecast time from 0 to 3 hours reproduced from the analyzed fields. Valid time is 15 to 18 JST 16 July 2004.

Heavy rainfall was not reproduced by assimilation of conventional data.

Rainfalls region predicted from analyzed fields (GPS data)

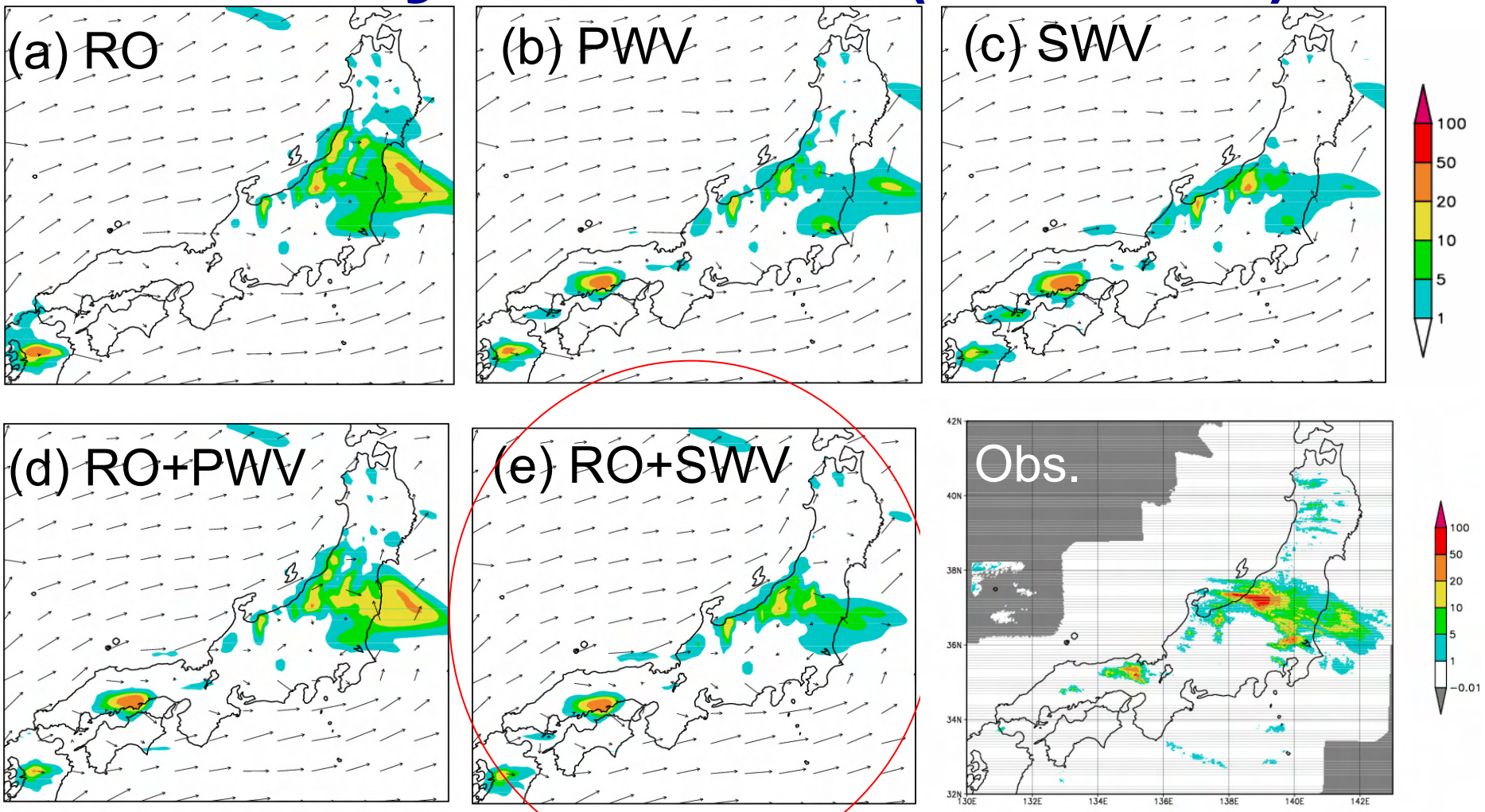

Reproduced 3-hour rainfall of forecast time from 0 to 3 hours reproduced from the analyzed fields. Valid time is 15 to 18 JST 16 July 2004.

Rainfalls region predicted from assimilated field of RO

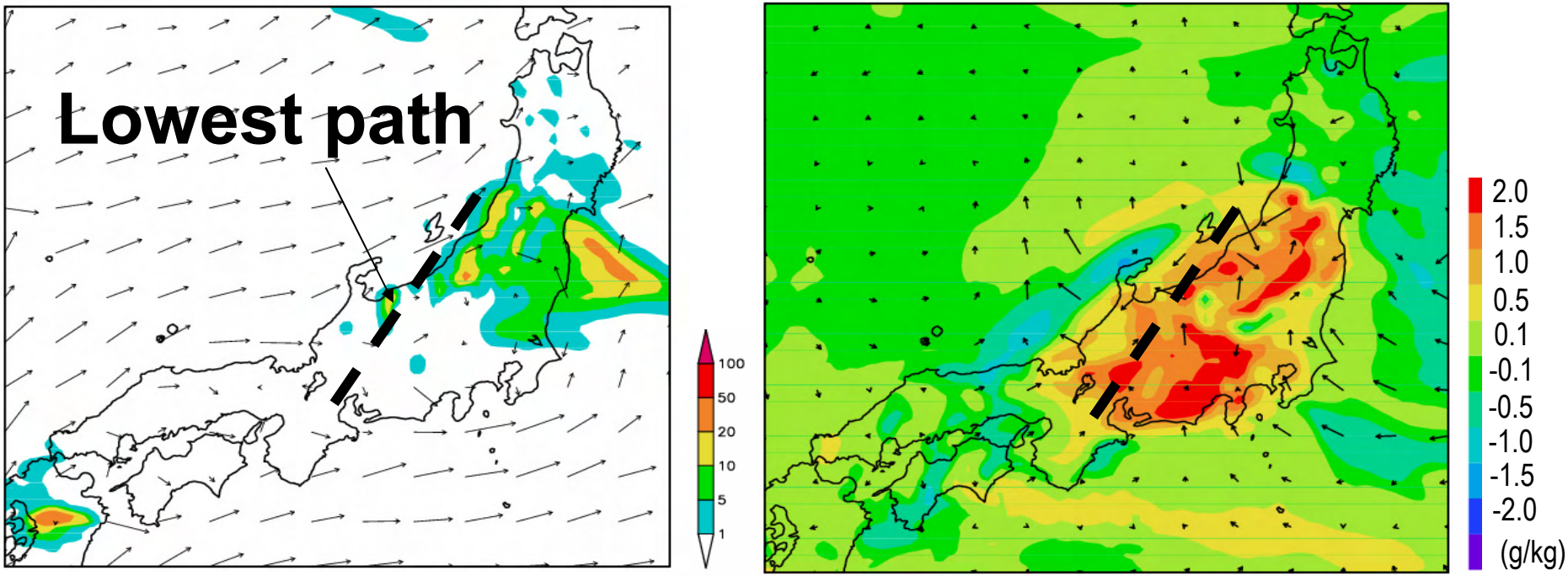

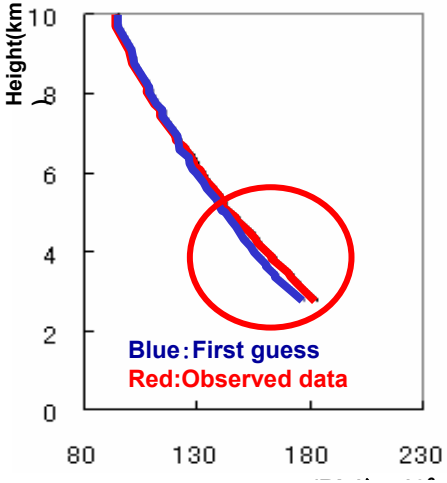

Reproduced 3-hour rainfall and increment of Qv

- **Rainfall was intensified as it is expected by the D-value of RI profile.**

Rainfalls region predicted from assimilated field of RO

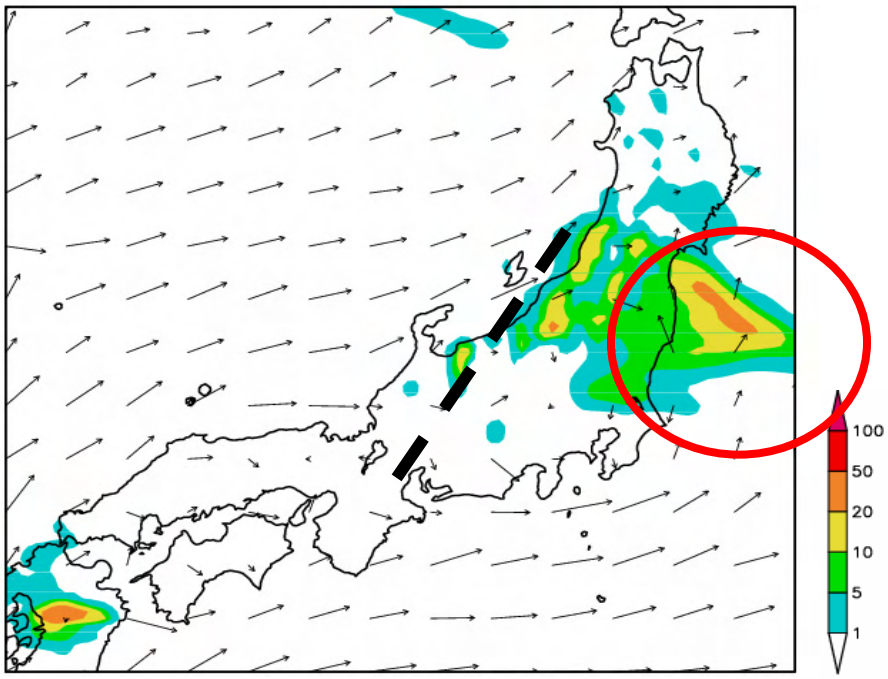

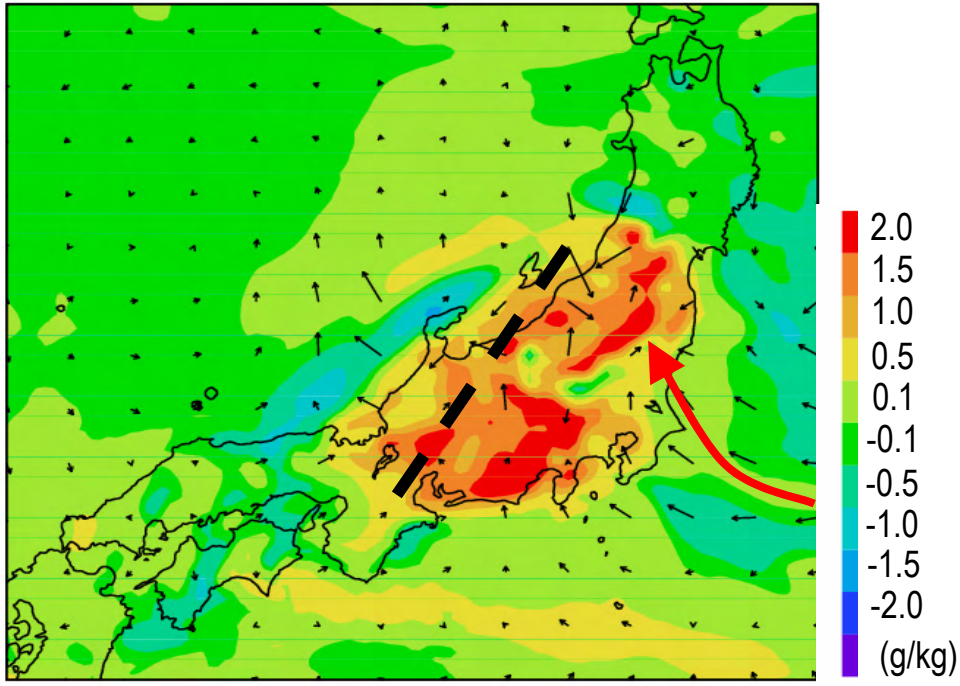

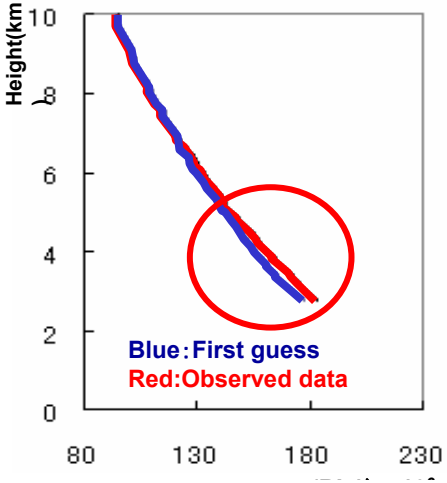

Reproduced 3-hour rainfall and increment of Qv

- **But, Eastern part is too strong.**
- **Moist SE-ly flow enhanced the intensity of the rainfall.**

Rainfalls region predicted from assimilated field of PWV

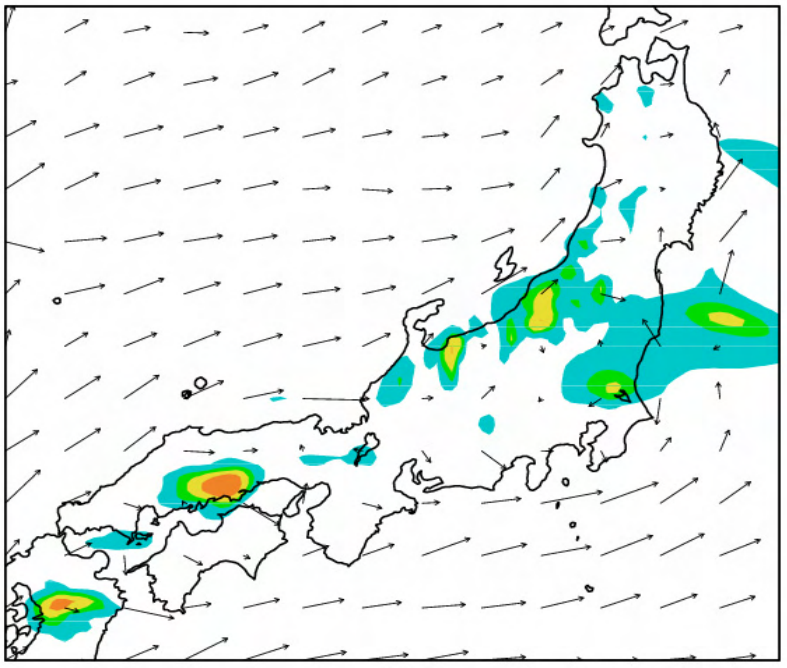

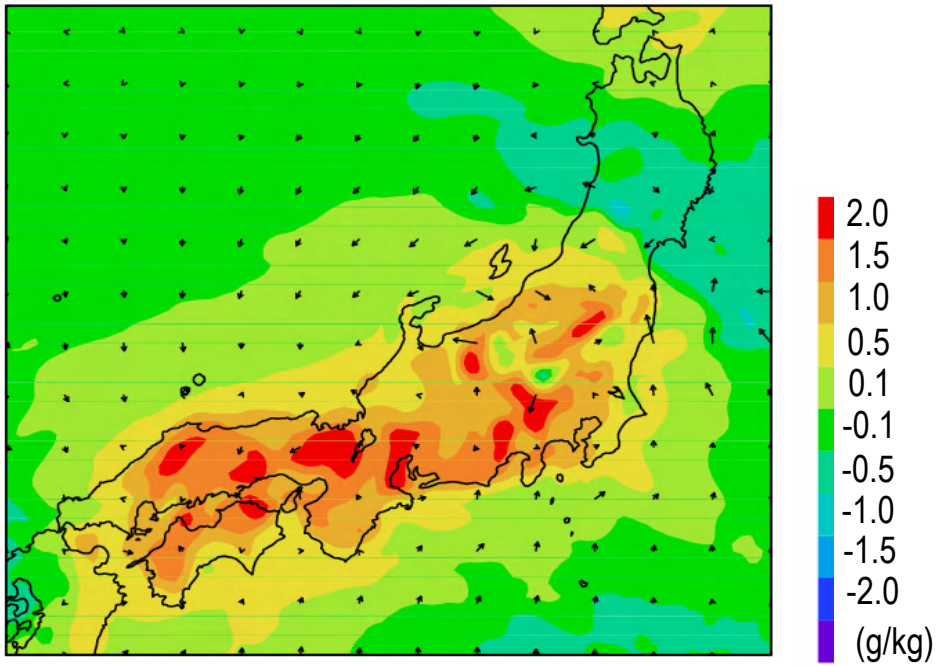

Reproduced 3-hour rainfall and increment of Qv

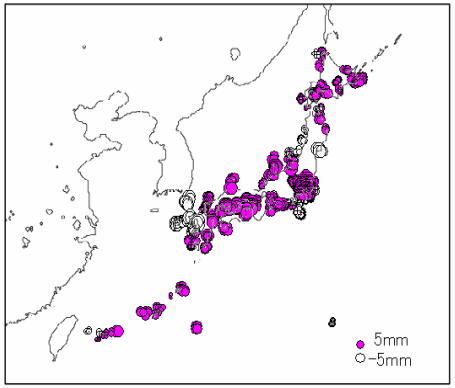

- **Rainfall was intensified as it is expected by the D-value distribution of ground-based GPS.**

Rainfalls region predicted from assimilated field of PWV

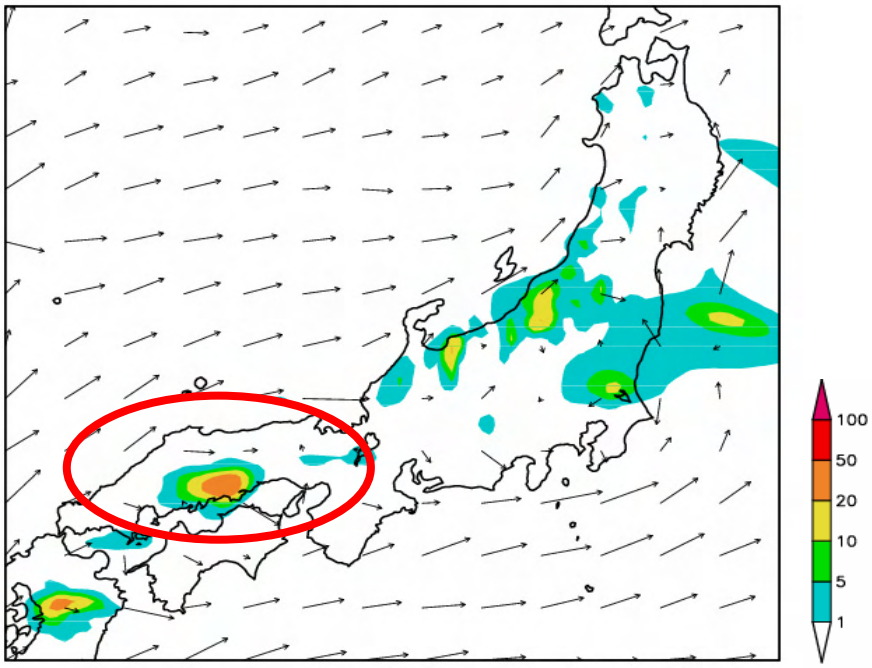

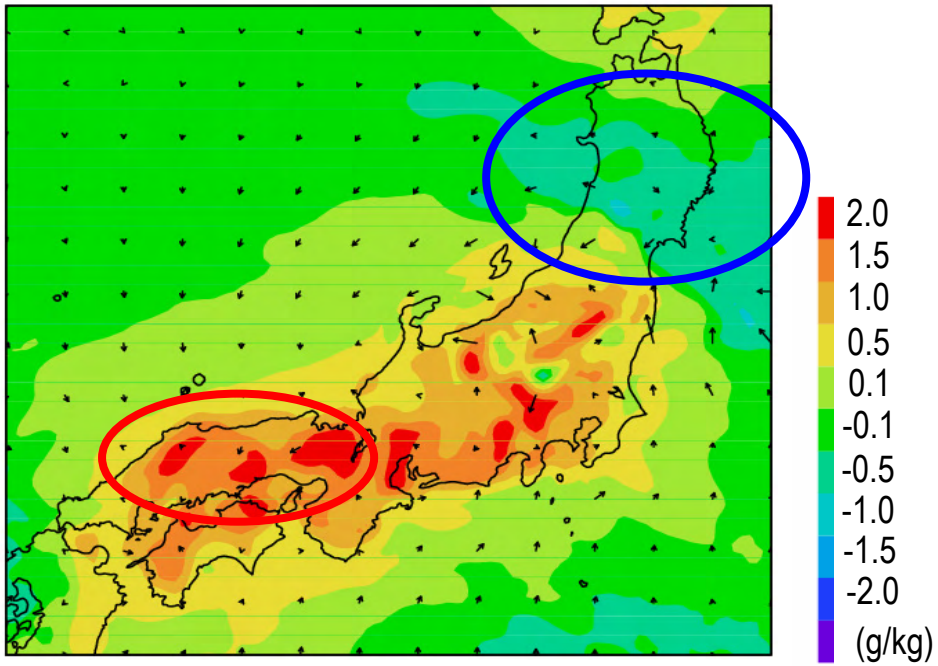

Reproduced 3-hour rainfall and increment of Qv

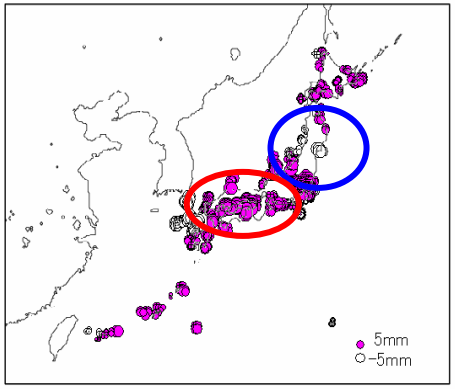

- **Increment of water vapor is consistent with d-value distribution.**

Rainfalls region predicted from assimilated field of PWV

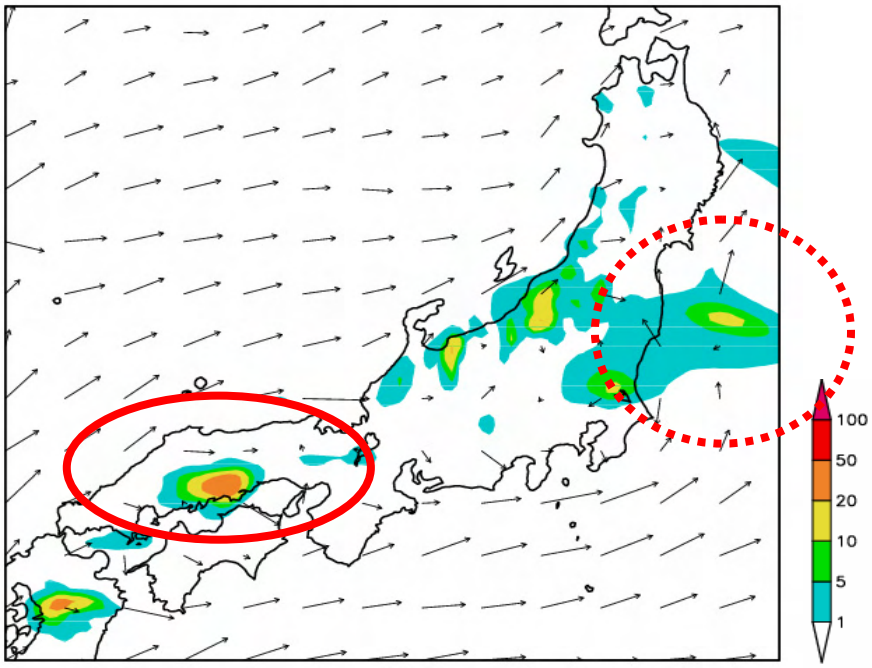

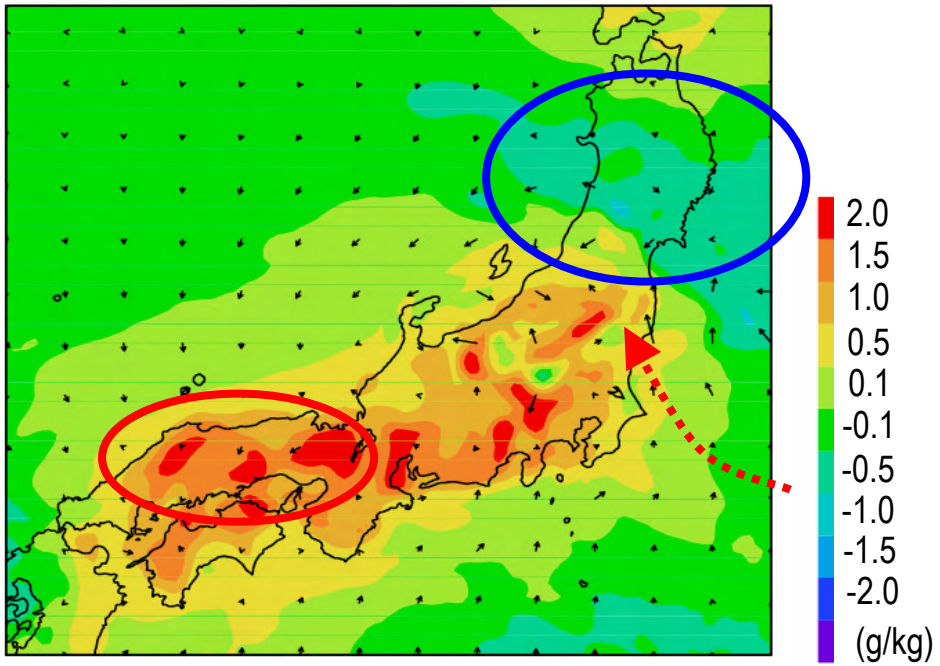

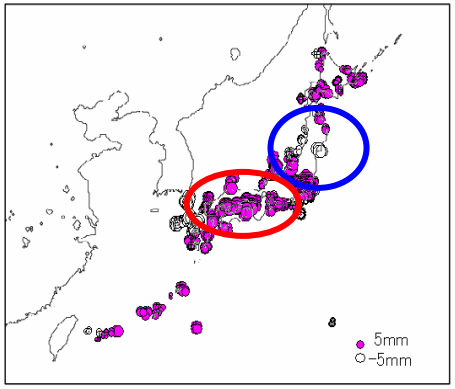

Reproduced 3-hour rainfall and increment of Qv

- **Eastern part was weaker than RO.**
- **Weak SE-ly flow reduced 3hour-rainfall, though water vapor was increased.**

Rainfalls region predicted from assimilated field of SWV

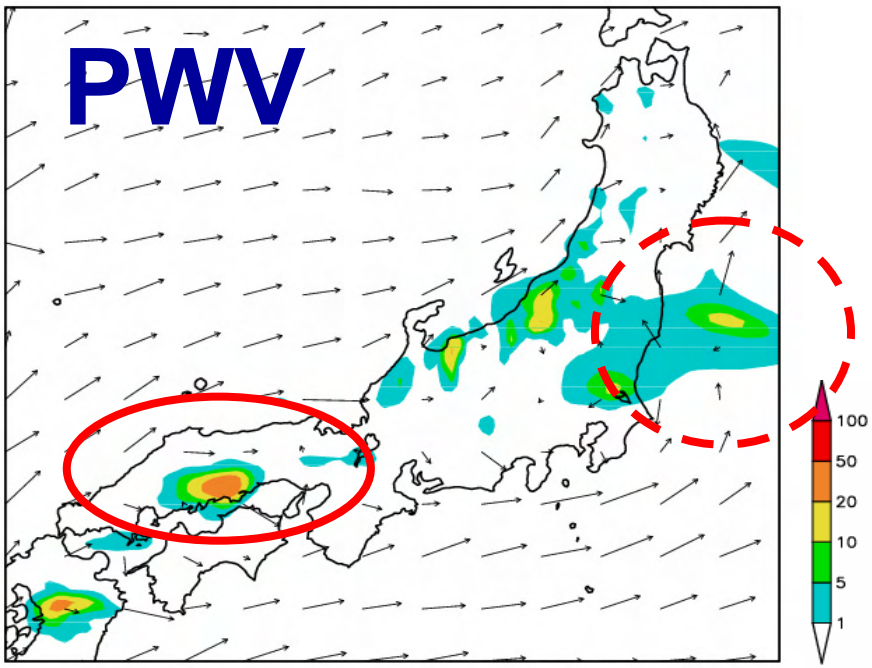

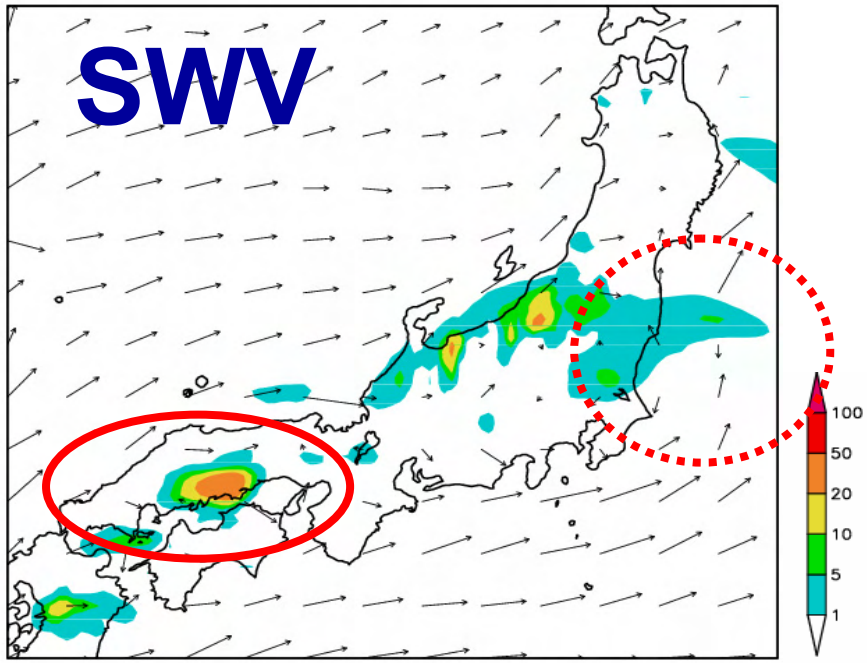

Reproduced 3-hour rainfall and increment of Qv

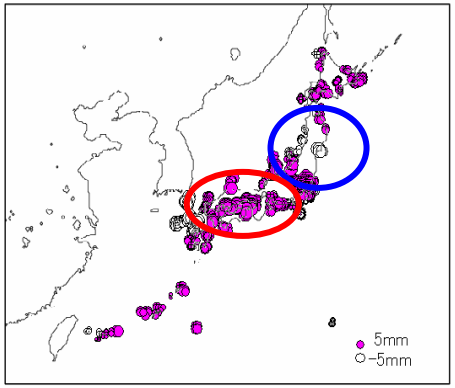

- **Eastern part of heavy rainfall was weaker.**

Rainfalls region predicted from assimilated field of SWV

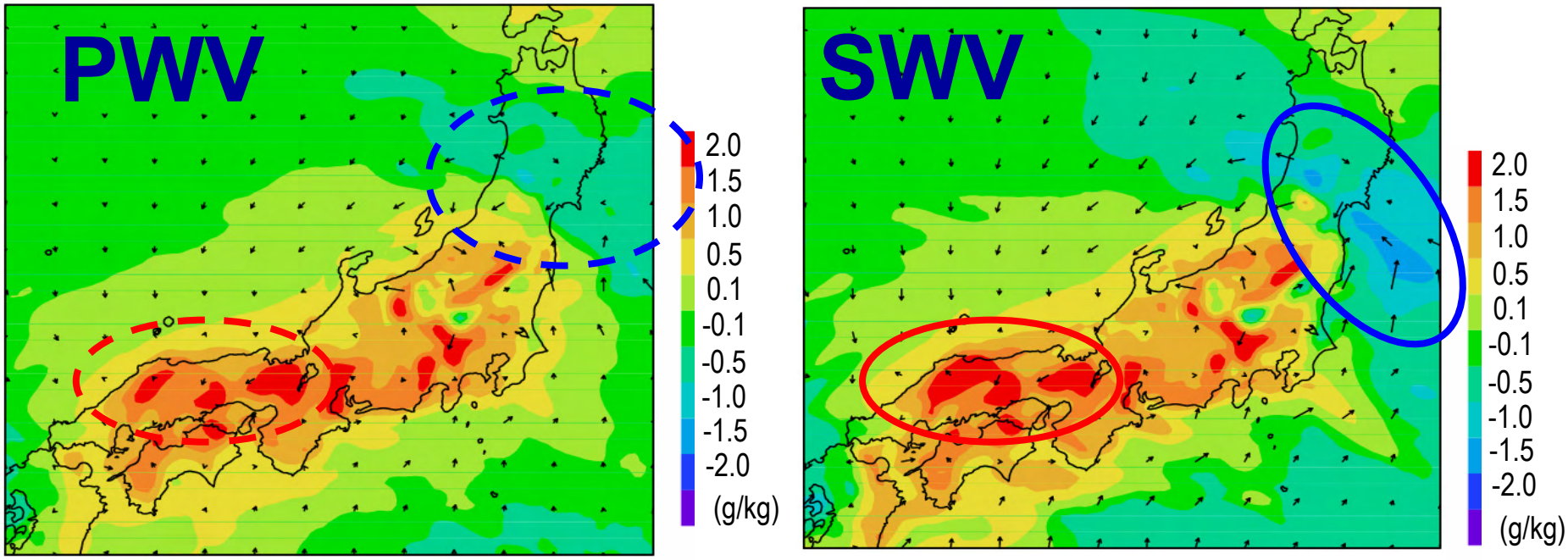

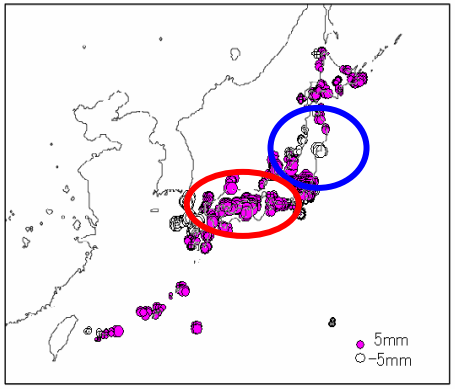

Reproduced 3-hour rainfall and increment of Qv

- **Increment became more significant when SWV was used.**
- **Water vapor on eastern side of northern Japan was decreased.**

Rainfalls region predicted from assimilated field of SWV

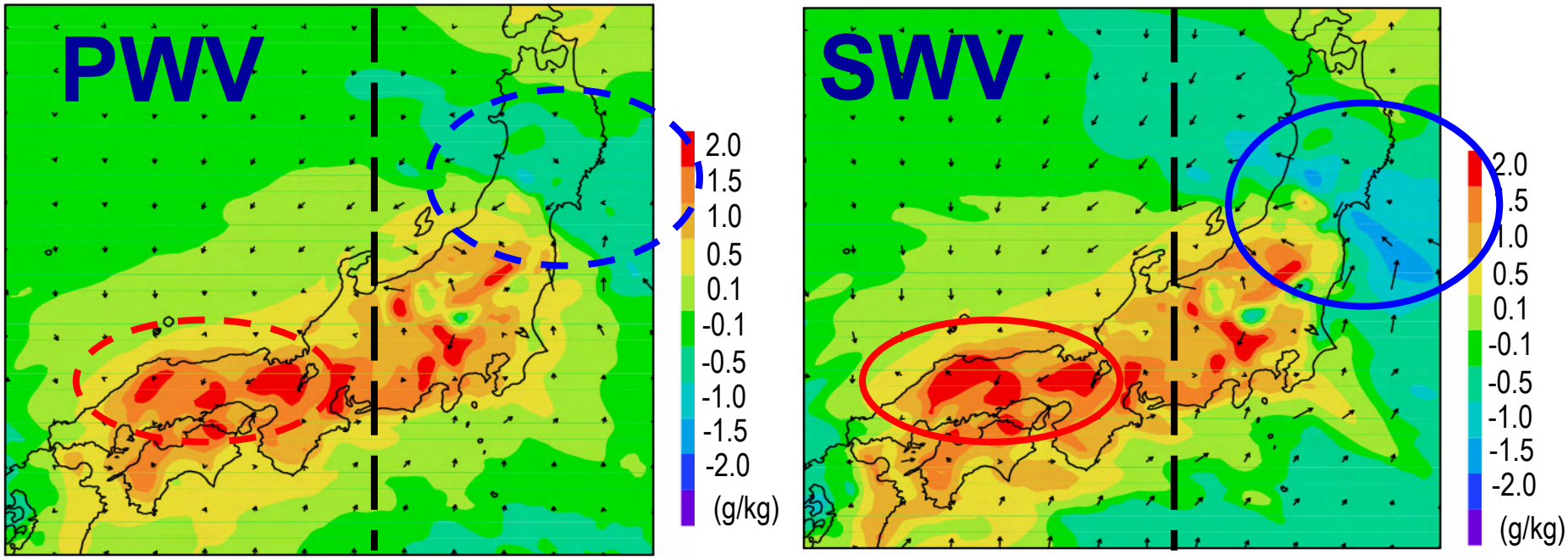

Reproduced 3-hour rainfall and increment of Qv

- **How are vertical cross sections modified?**

Vertical distribution of increments of water vapor

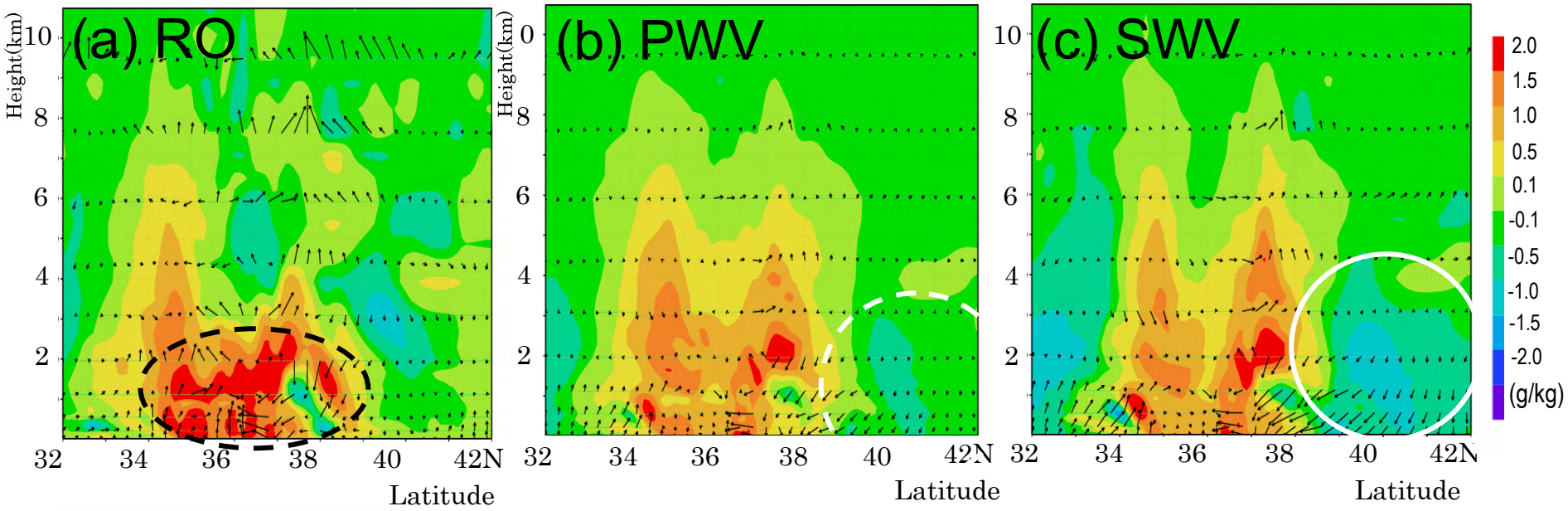

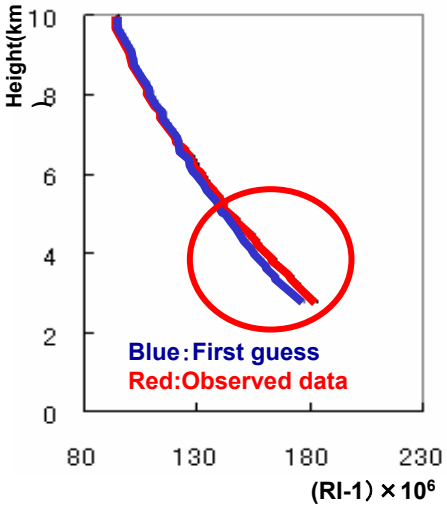

- When RO data was assimilated, water vapor was increased at the low-level.
- SWV modified the vertical distribution, but not so large.

Synergistic improvement using RO and ground-based GPS data

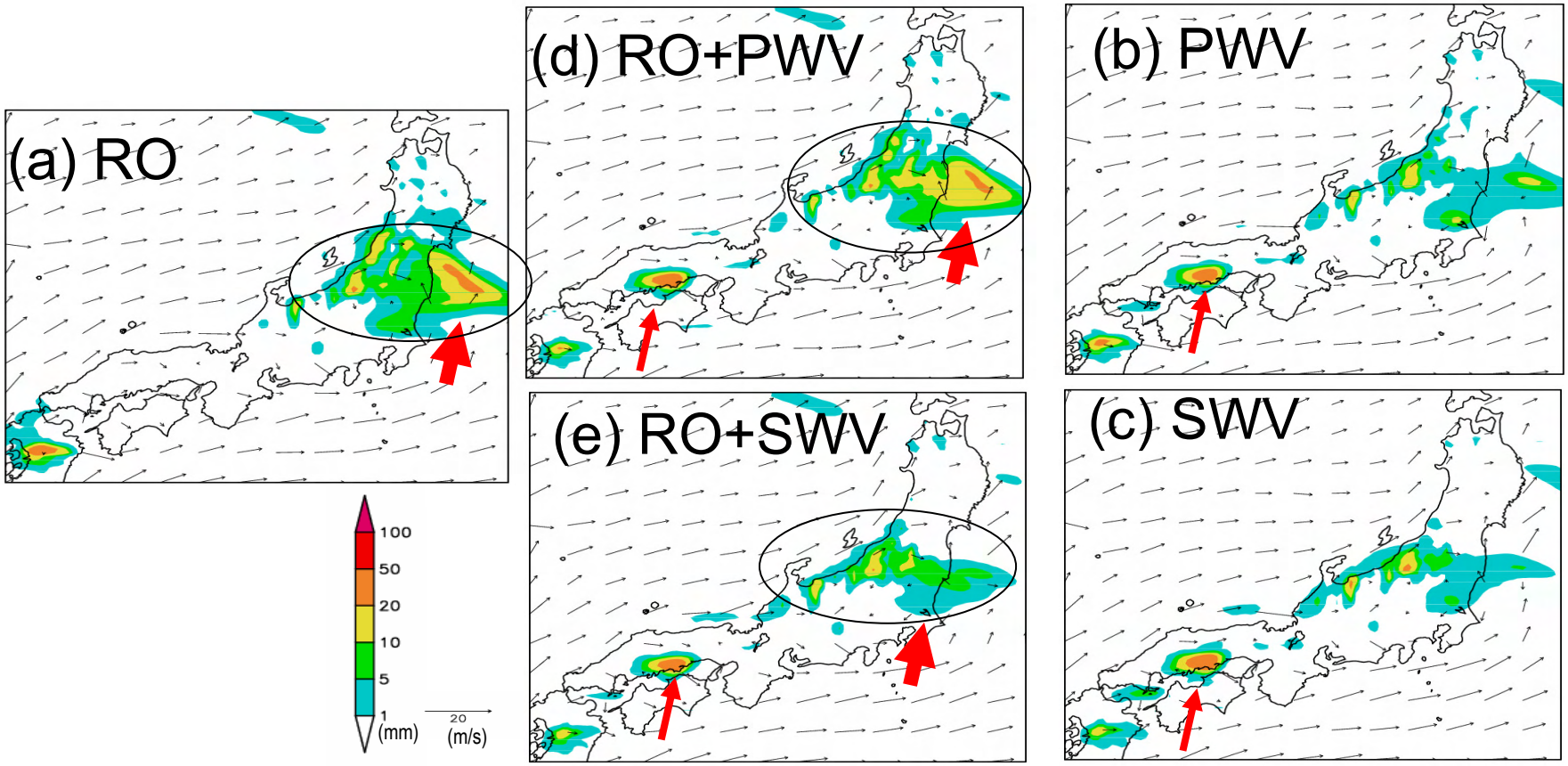

- When both data were assimilated, the rainfall regions had both features of RO and ground-based GPS data.

Synergistic improvement using RO and ground-based GPS data

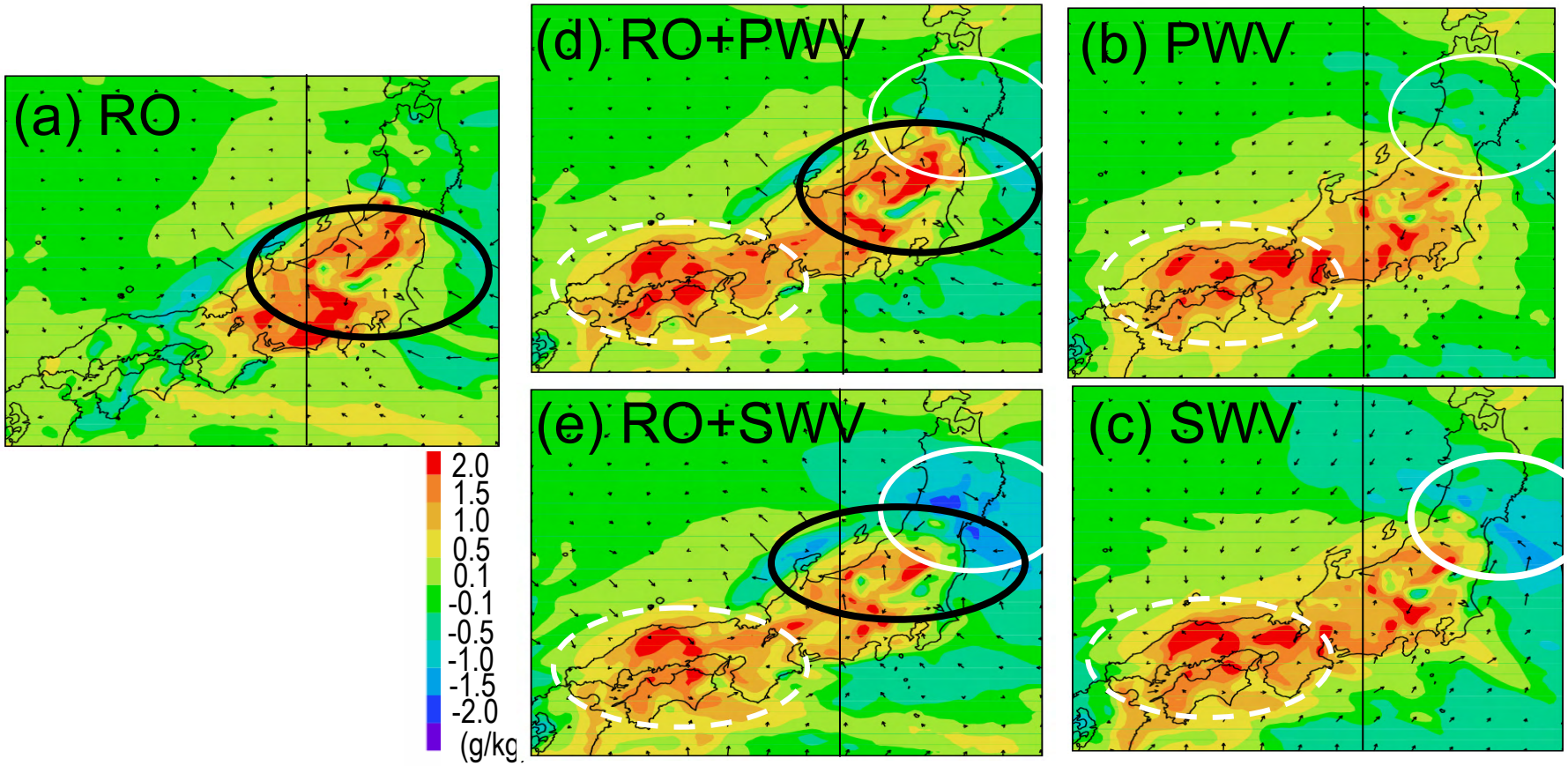

- When both data were assimilated, the increments had both features of RO and ground-based GPS data.

Synergistic improvement using RO and ground-based GPS data

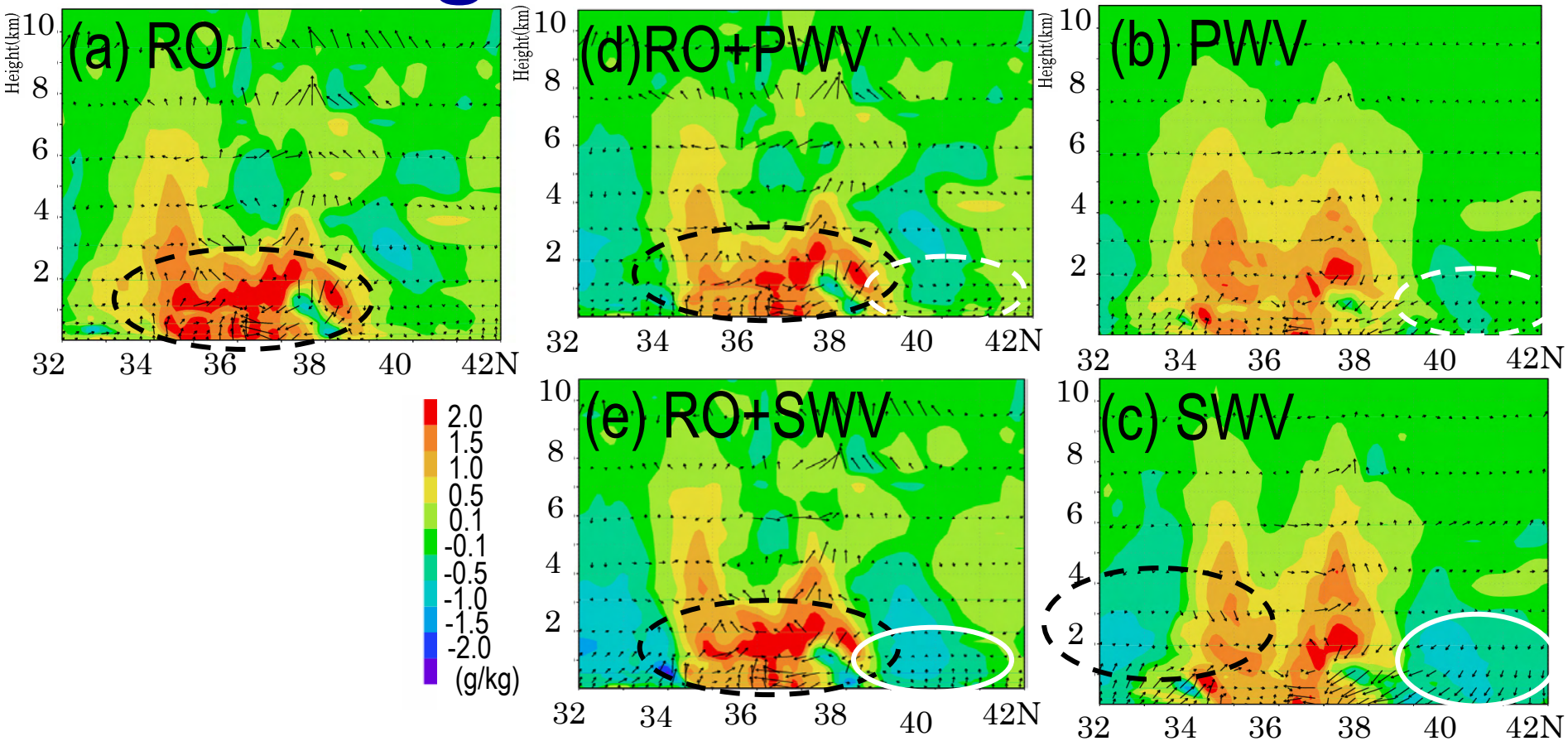

- When both data were assimilated, the increments had both features of RO and ground-based GPS data.

Synergistic improvement using RO and ground-based GPS data

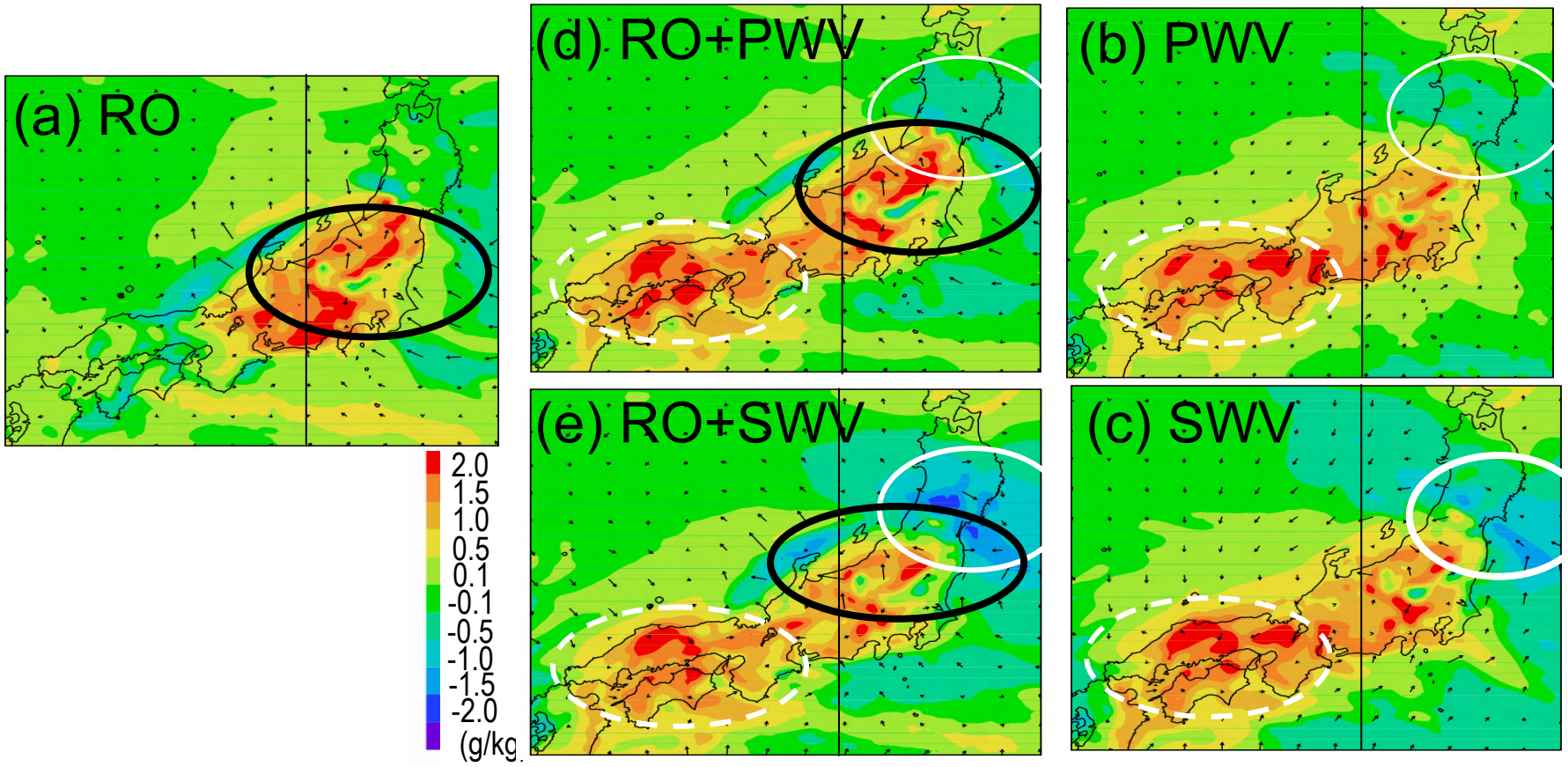

- When RO and SWV data were assimilated, the rainfall region was most similar to the observed one.

Synergistic improvement using RO and ground-based GPS data

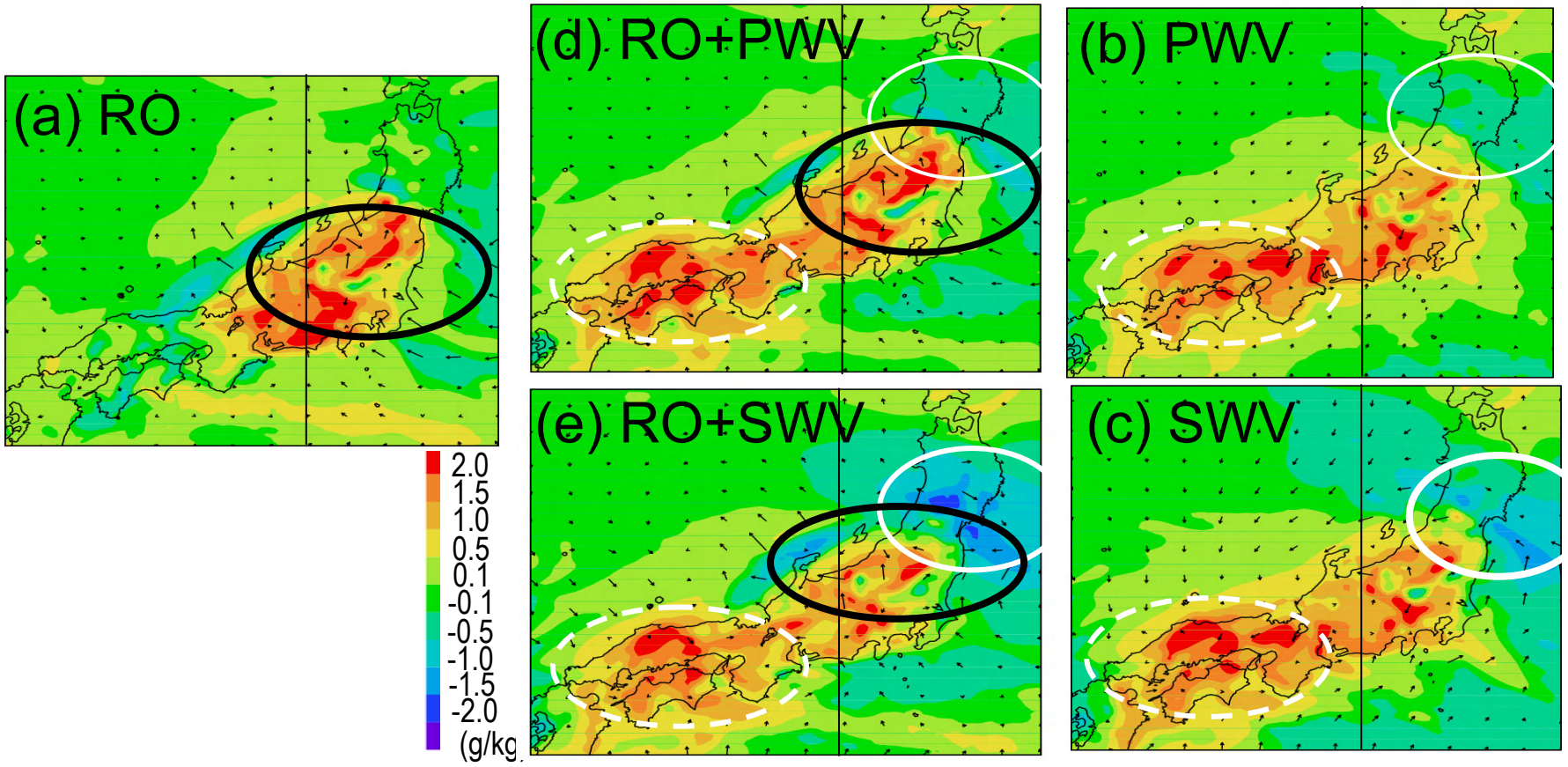

- **Simultaneous assimilation of RO and ground-based GPS data improves the forecast of the heavy rainfall effectively.**

•Summary of synergistic improvement

- **Assimilation method of path data was developed. In this method, the vertical correlation of observation error was considered.**
- **When RO data and ground-based GPS data are assimilated simultaneously, rainfall forecast and water vapor fields are much improved.**

3. Impacts on the development of the typhoon USAGI (0705)

(Kunii et al. 2010)

3a. Results of assimilation of GPS RO data

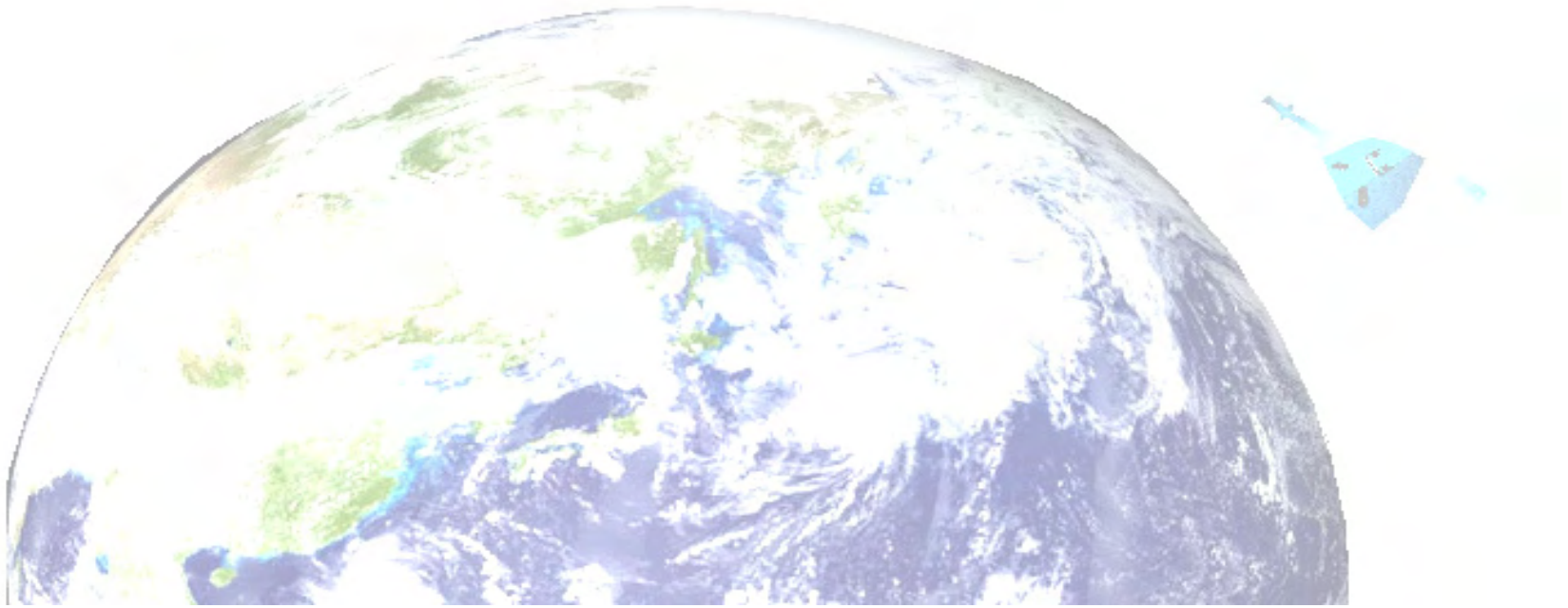

Typhoon USAGI (0705)

Best track

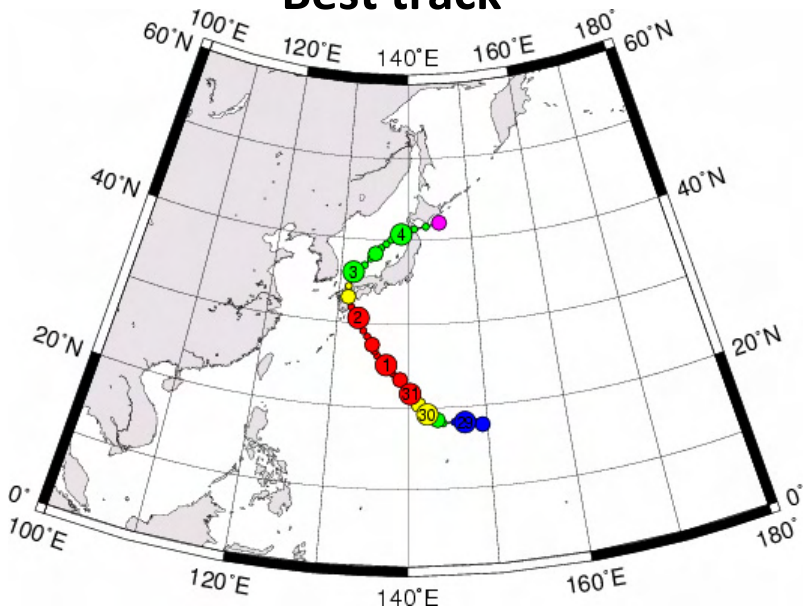

Central Pressure

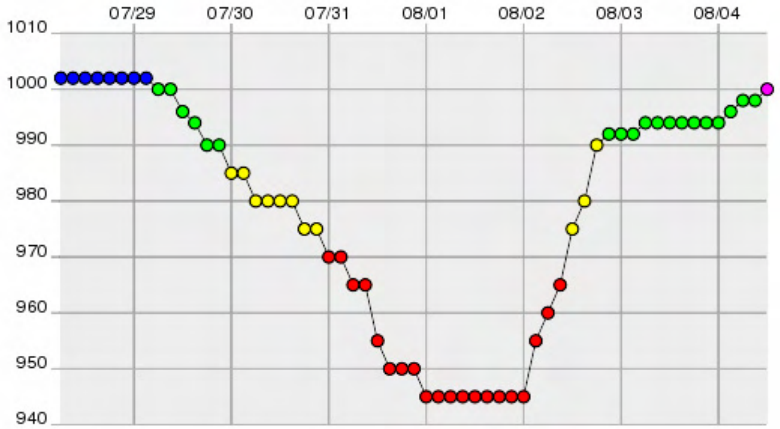

Basic Information	
Birth	2007-07-29 06UTC
Death	2007-08-04 06UTC
Lifetime	144 hours
Min. Pressure	945 hPa
Max. Wind	90 knots

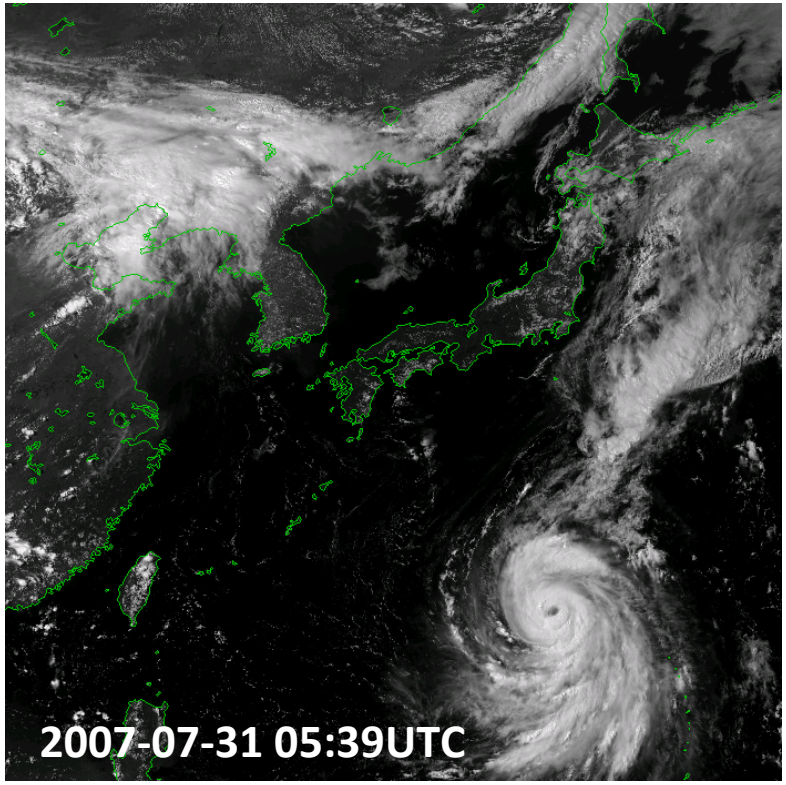

GSM Forecast Result

Valid : 2007/07/30 00UTC (BST : 19.2N 142.5E, 985hPa)

ANAL

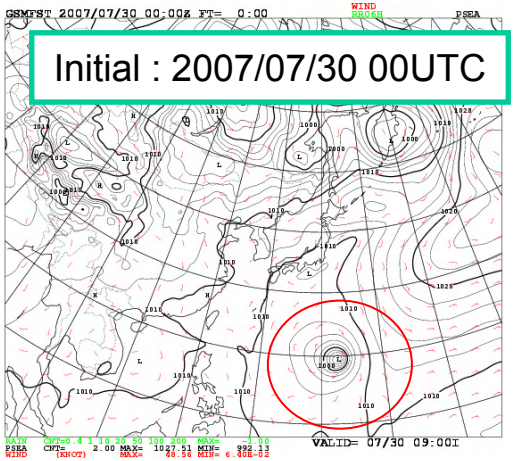

FT=12

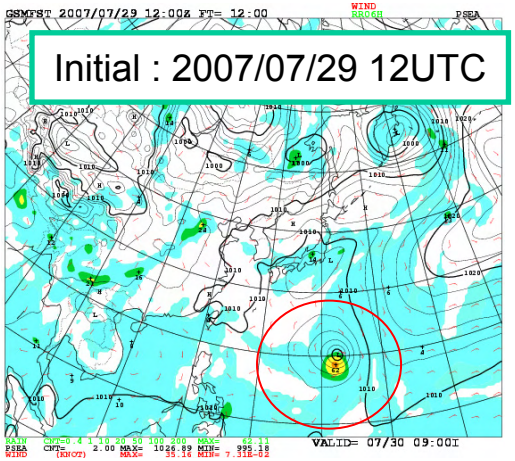

FT=24

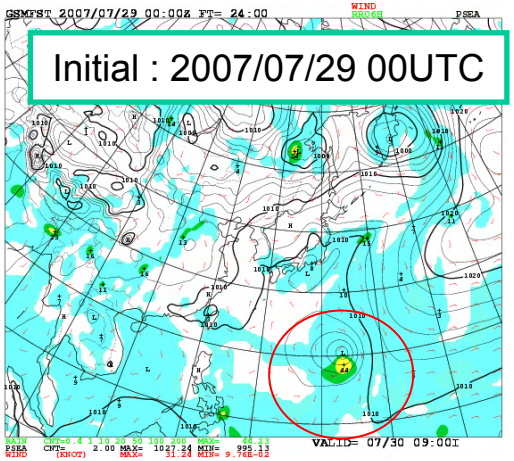

FT=36

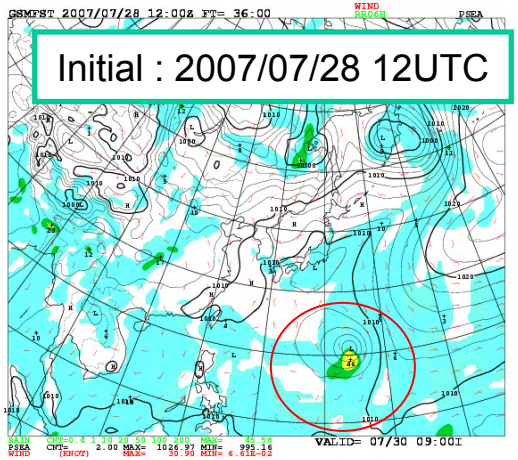

FT=48

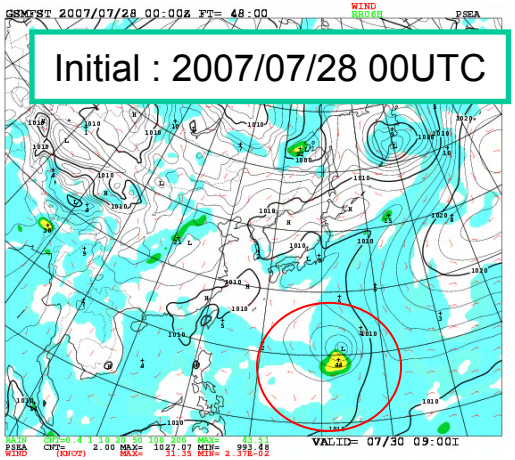

FT=60

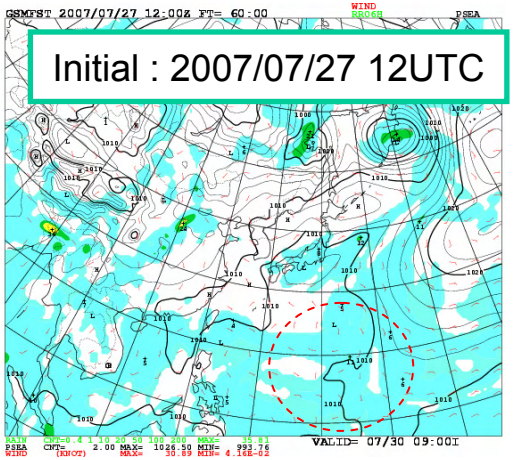

We searched the initial in which typhoon was not predicted.

GSM Forecast Result

Valid : 2007/07/30 00UTC (BST : 19.2N 142.5E, 985hPa)

ANAL

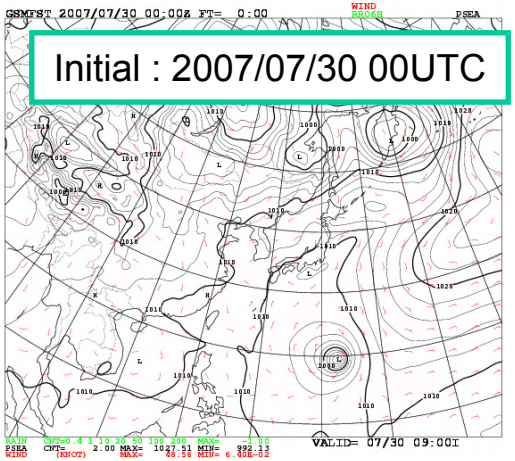

FT=12

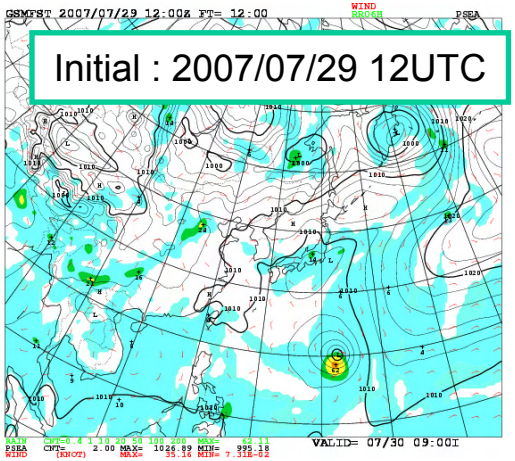

FT=24

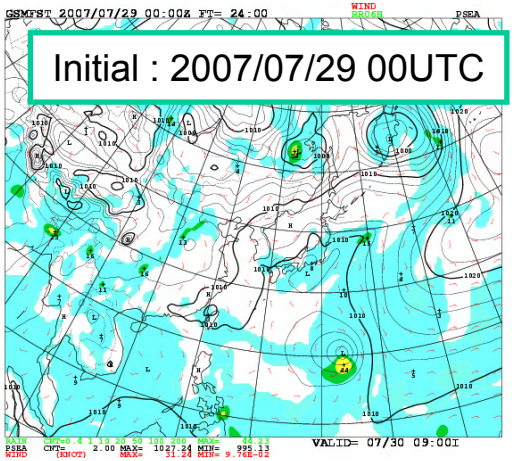

FT=36

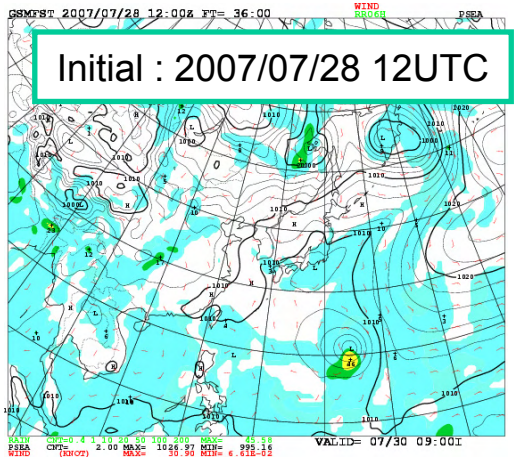

FT=48

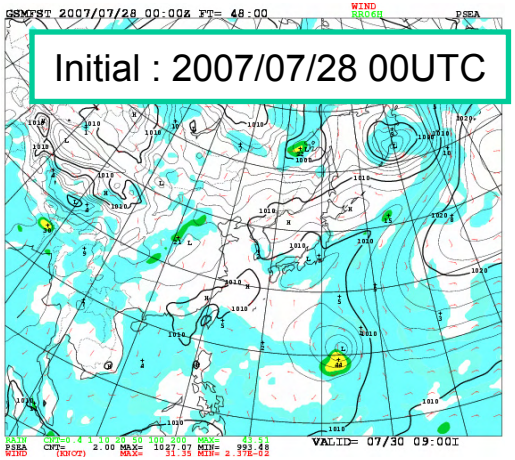

FT=60

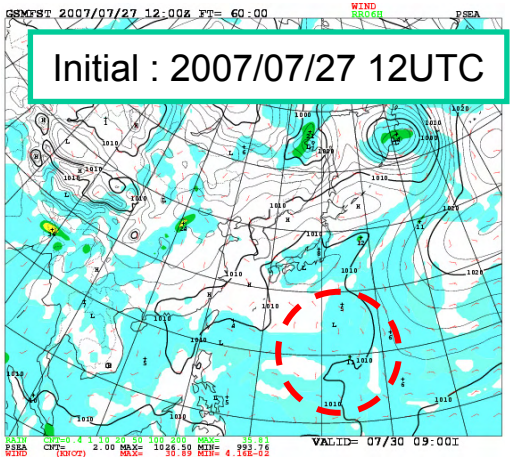

Initials before 07/27 12UTC was used as the first guess.

Data assimilation experiment

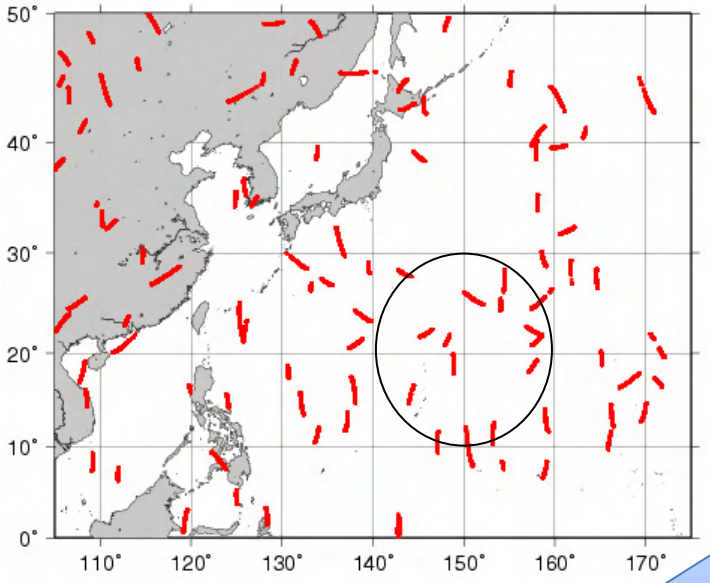

COSMIC data

distribution at 2007.7.26

1. GA

Use GSM 4D-Var Analysis

OUTER : Δx = 60km

INNER : Δx = 110km

2. MA

Use Meso 4D-Var Analysis

3. MA_RO

Use Meso 4D-Var Analysis
(with COSMIC RO data)

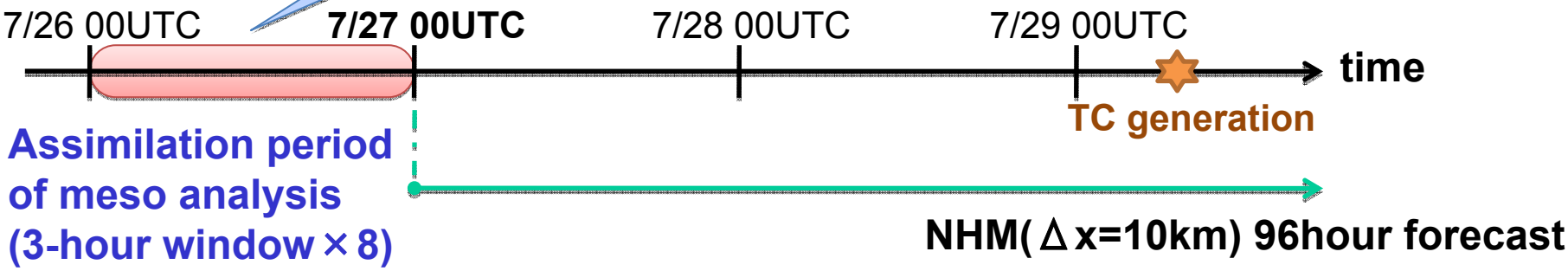

Impact of GPS RO (1st window)

Analysis increments (MA_RO - MA) at the initial time of the first window in the 24-hour assimilation period (00 UTC 26 July).

Qv (MA_RO-MA)

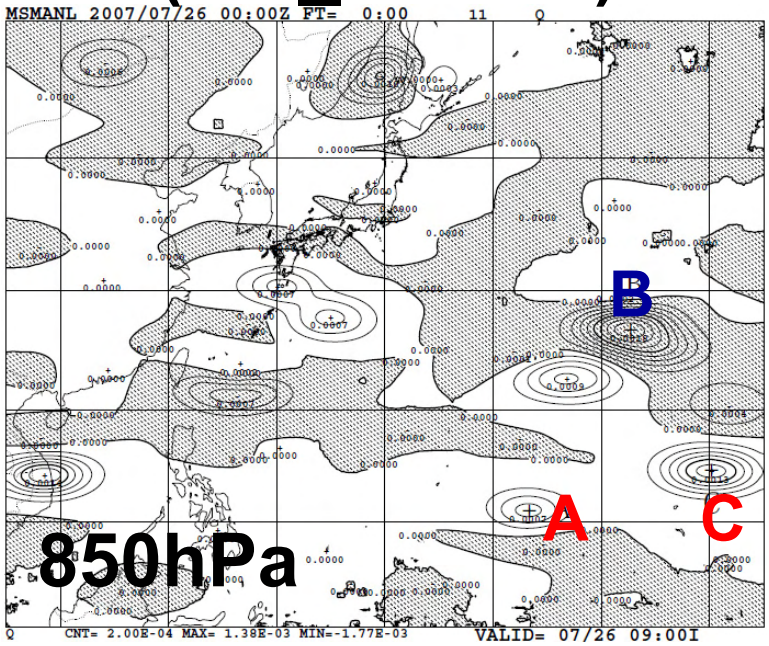

Figure. Horizontal distribution of the difference in mixing ratio of water vapor at z=11 (≒850 hPa) between MA_RO and MA at 00 UTC 26 July 2007. Hatched area denotes area of negative increment.

Qv(100km from obs. points)

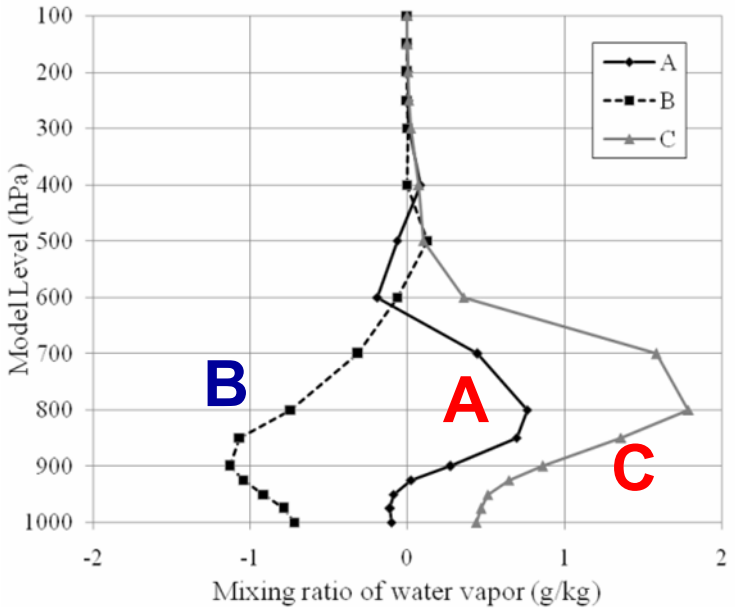

Figure. (a) Vertical profiles of the difference in mixing ratio of water vapor between MA_RO and MA averaged within a circle with a radius of 100 km centered on the individual observational point between 00 UTC and 03 UTC on 26 July 2007.

Impact of GPS RO data (analysis)

The difference of moisture field at initial time of the subsequent model forecast (00 UTC 27 July)

RH (1000km from vortex)

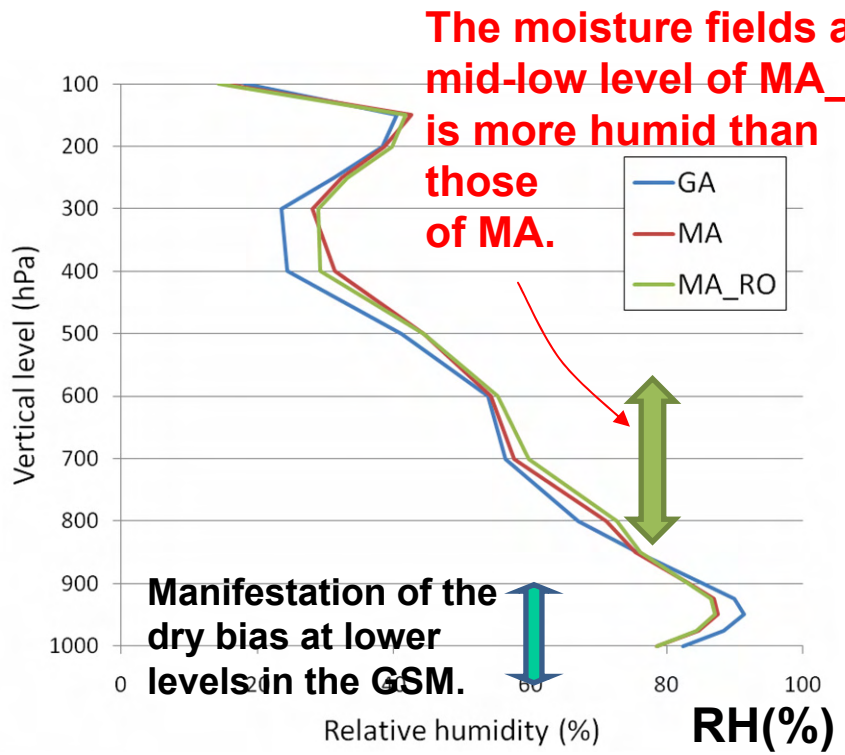

RH (MA_RO-MA)

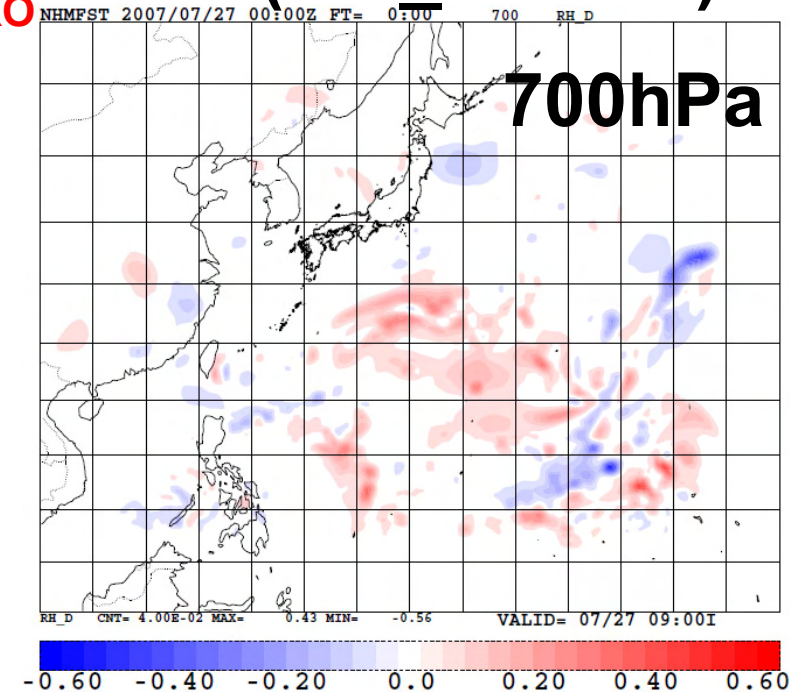

The moisture fields at mid-low level of MA_RO is more humid than those of MA.

Forecast Result

Ps and 3-hour rainfall (FT=00 - 96)

GA

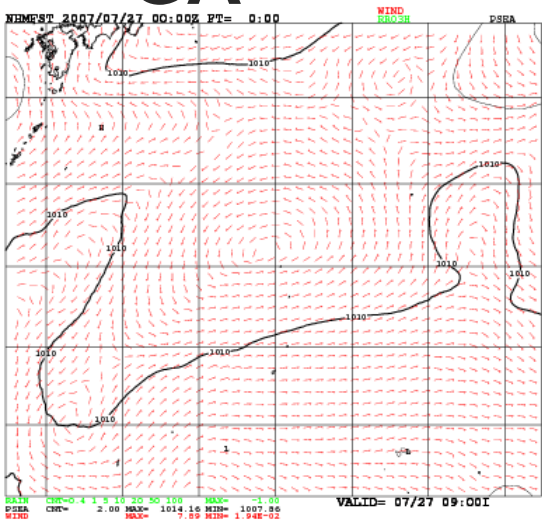

MA

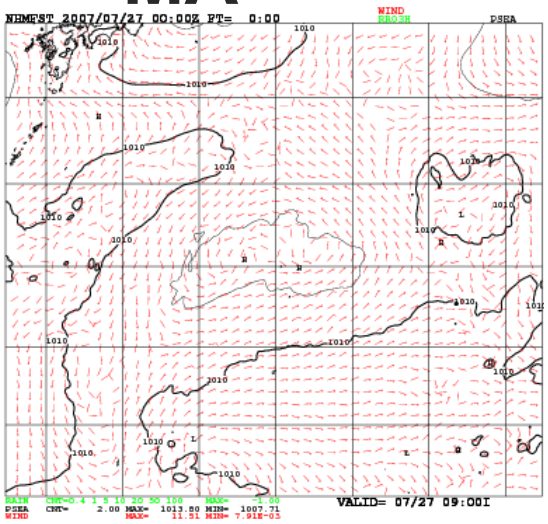

MA_RO

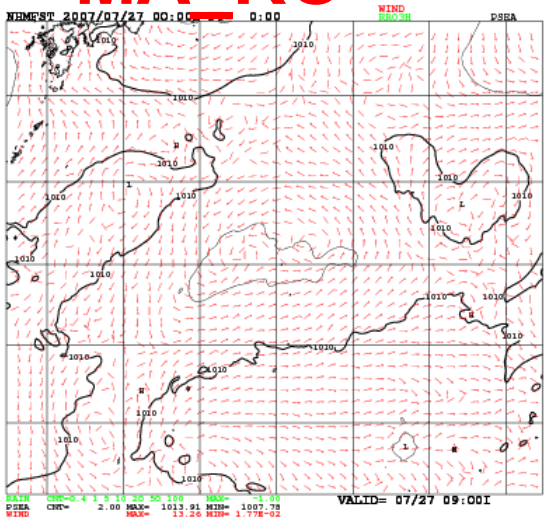

GSM Forecast

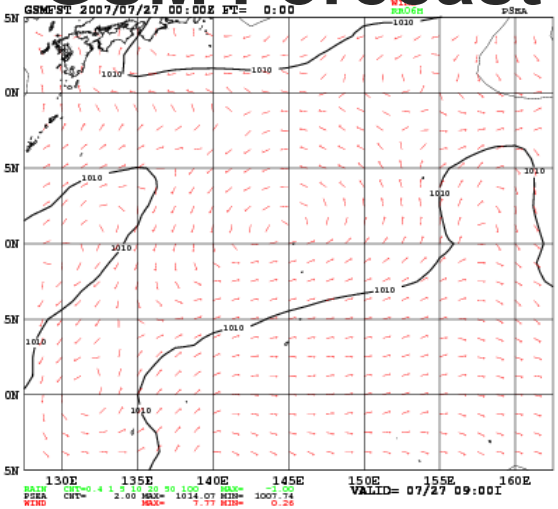

When the global analysis is used for the initial field, the typhoon is not formed in the forecast model.

By contrast, when the global analysis is replaced by the meso 4D-Var analysis in the experiment, the generation of the typhoon is successfully simulated.

Forecast Result (Rainfall distribution)

Distributions of 3-hour Rainfall (at 00 UTC 31).

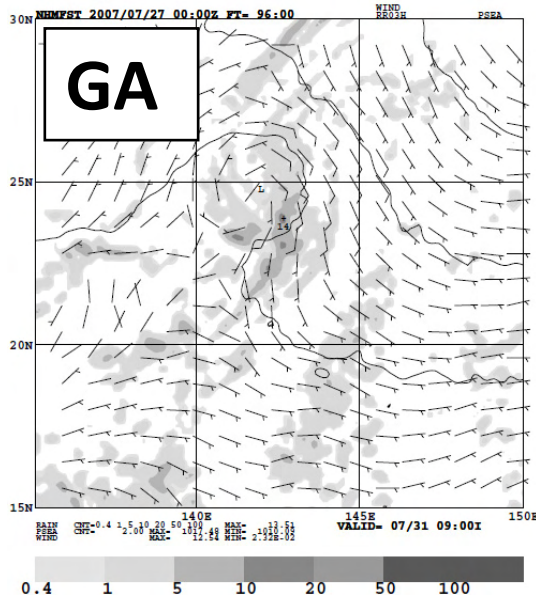

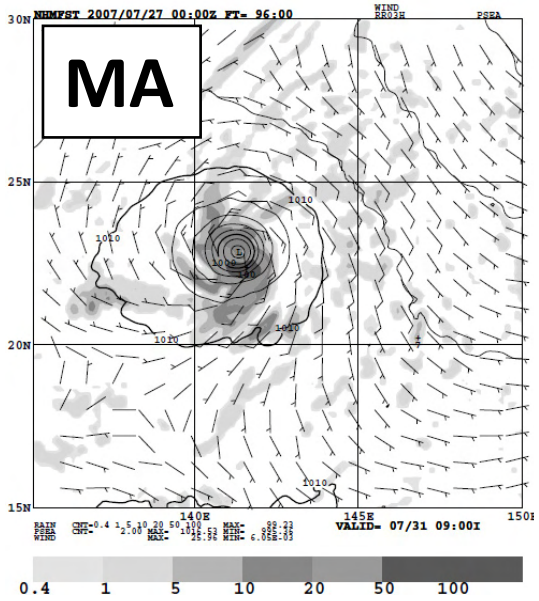

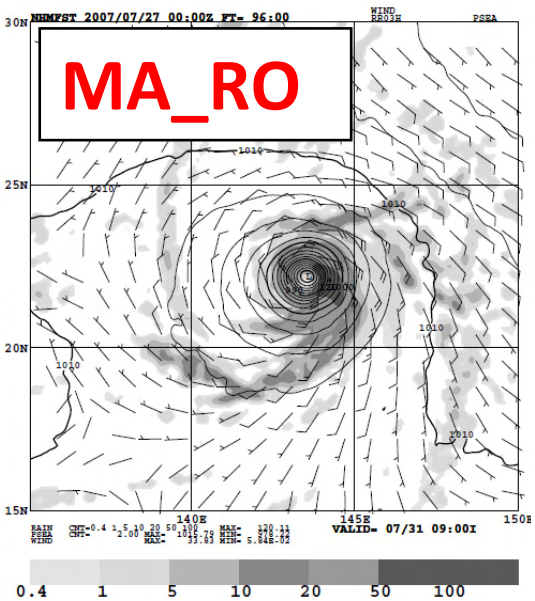

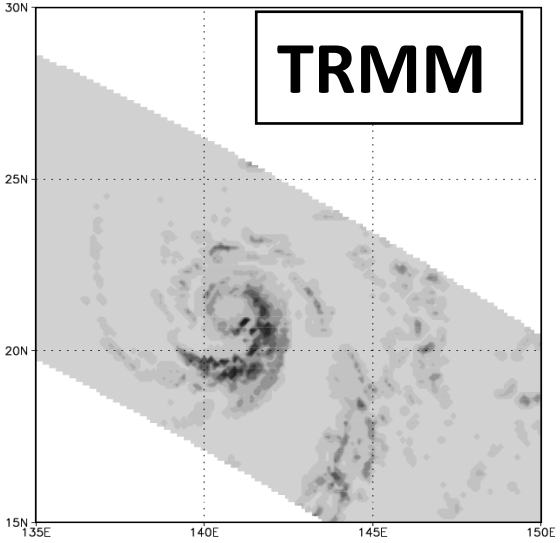

The shape of the major rain-band elongated from east to south of the cyclone center is comparatively well captured by MA_RO.

1-hour accumulated precipitation observed by **TRMM/TMI at 1732 UTC 30 July.**

Typhoon central pressure

With GPS refractivity assimilated, the simulated typhoon intensity is closer to the best-track data.

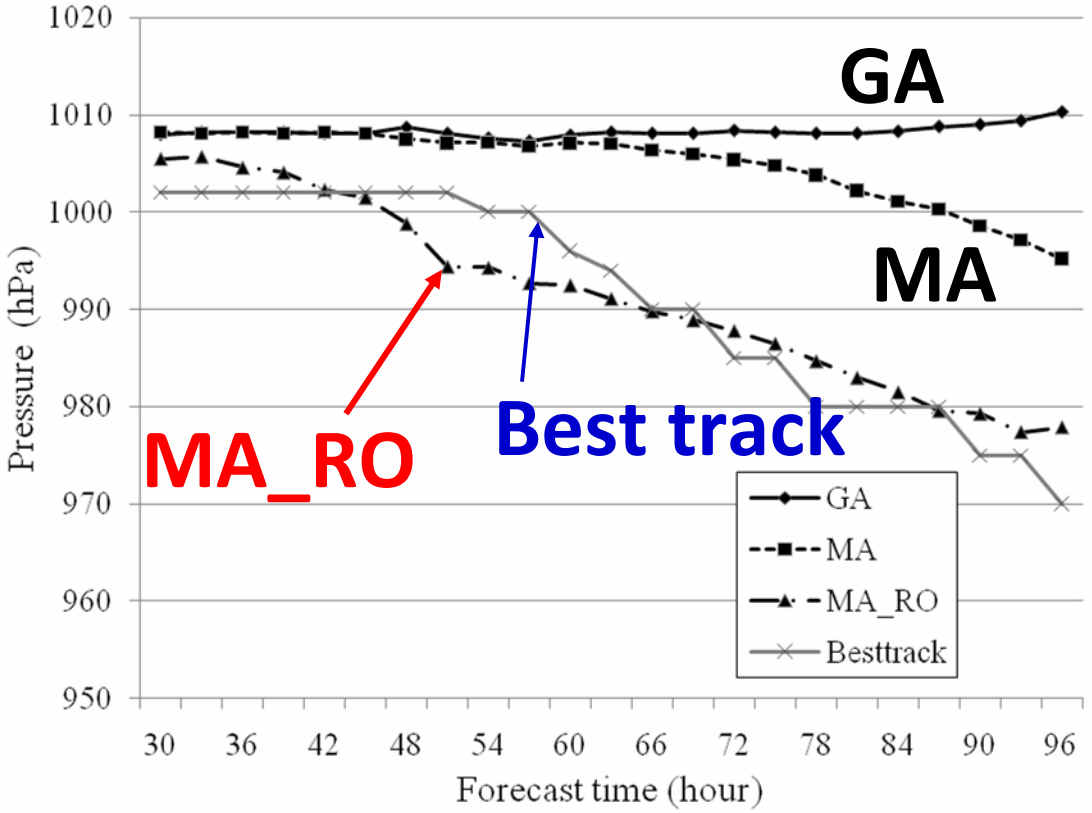

Figure. Time series of the central pressure of the typhoon Usagi predicted by the NHM.

PWV and AVOR

PWV and the absolute vorticity (AVOR850) from 200km from the Typhoon center

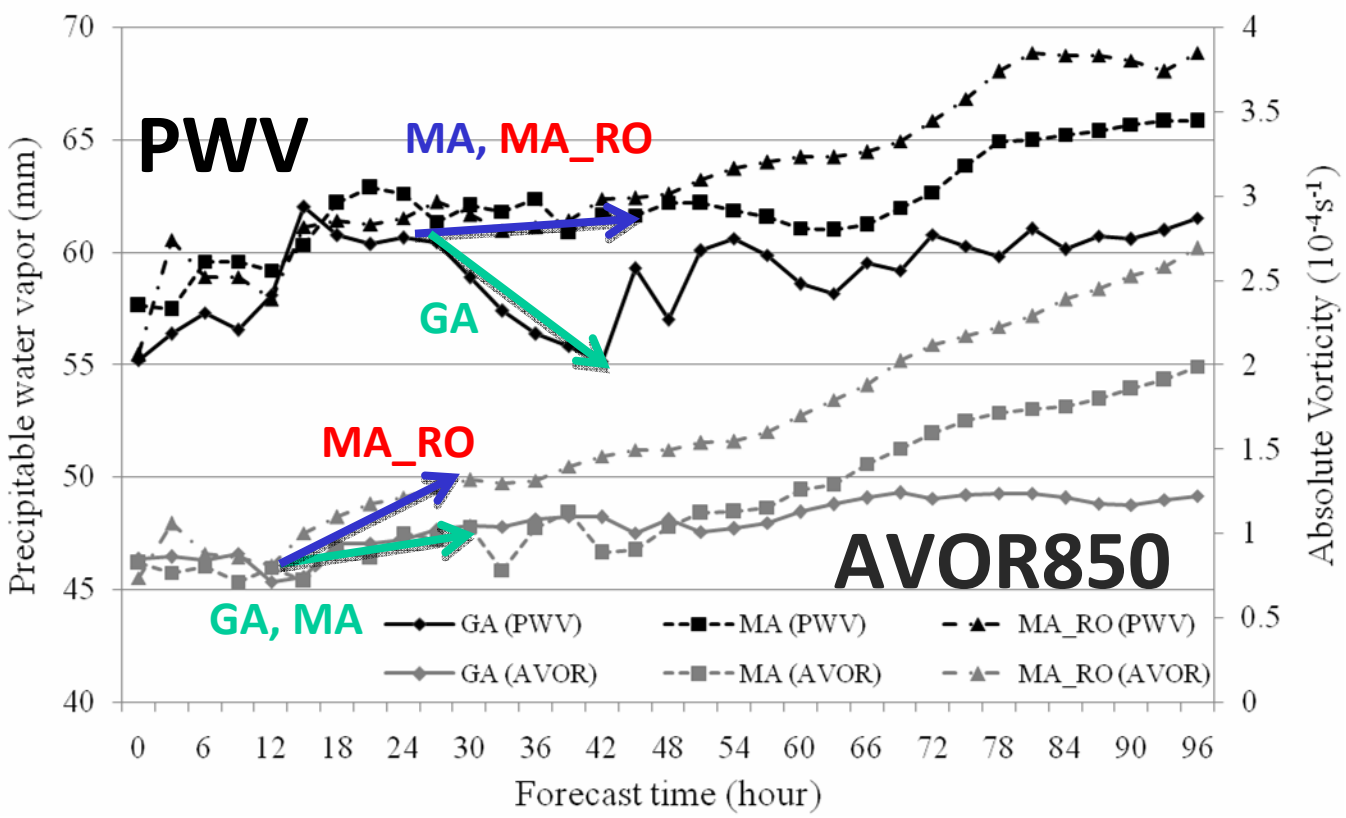

Figure. Time series of precipitable water vapor and absolute vorticity averaged within a circle with a radius of 200 km centered on the individual moving typhoon center for each experiment. Black lines indicate precipitable water vapor (PWV), and gray lines indicate absolute vorticity (AVOR) at 850 hPa level.

Vertical Wind Shear (FT=12)

(12 UTC 27 July)

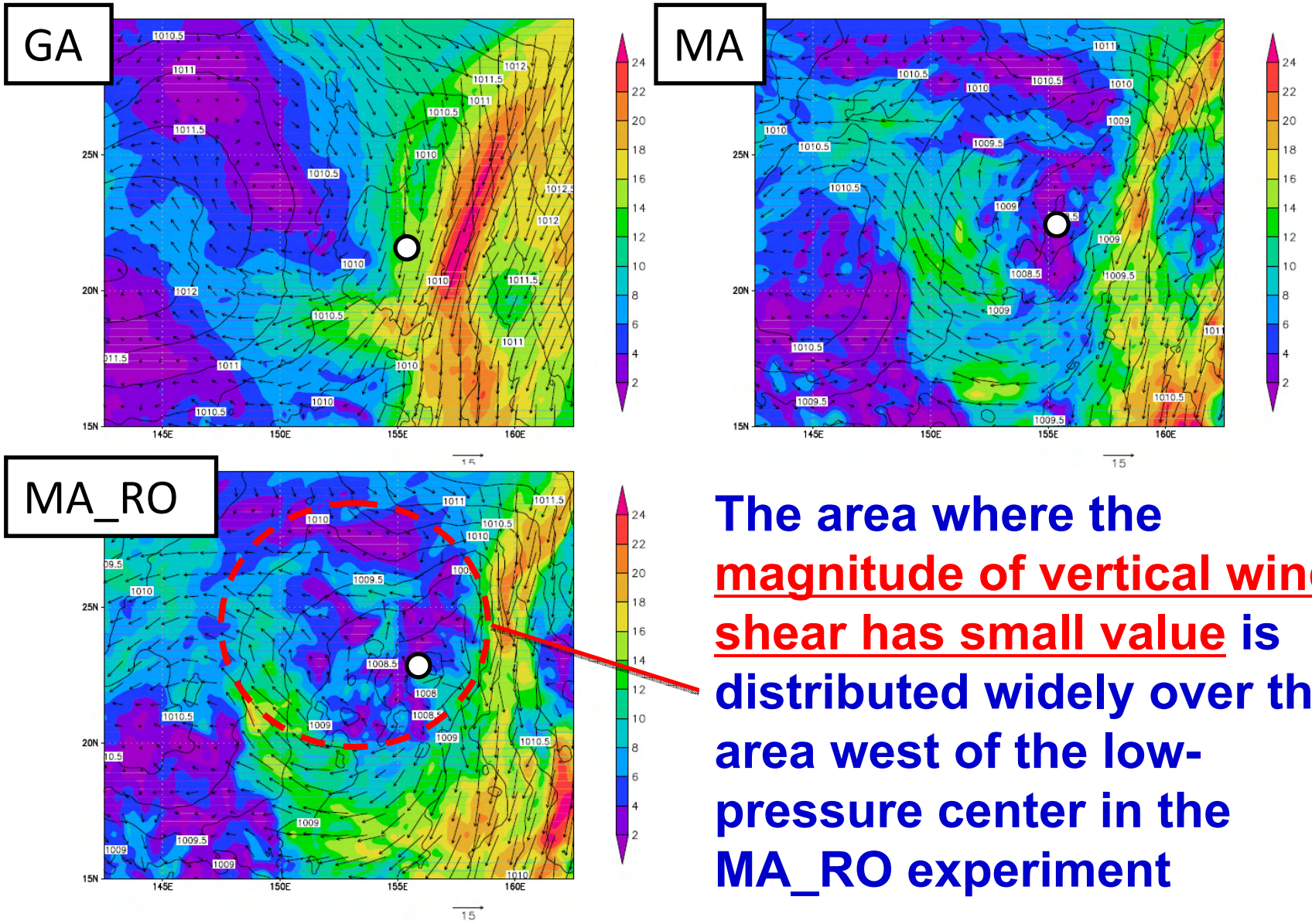

The area where the magnitude of vertical wind shear has small value is distributed widely over the area west of the low-pressure center in the MA_RO experiment

Summary of Impacts on the typhoon 0705.

- The assimilation system in low latitudes performs well and the generation of the typhoon is successfully simulated.
- With GPS refractivity assimilated, the simulated typhoon intensity is closer to the best-track data.

Thank you for your time

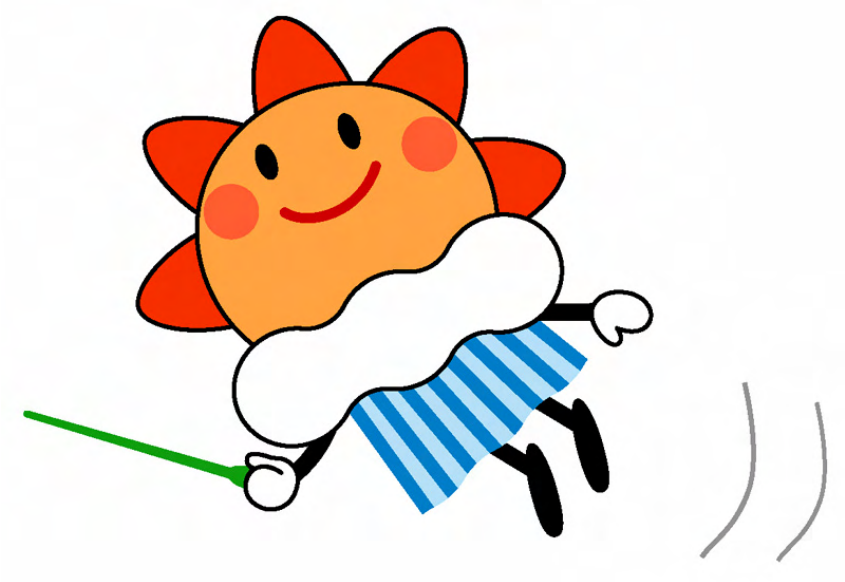

Acknowledgements

CHAMP, COSMIC and ground-based GPS data were provided from the GFZ, UCAR, NSPO and GSI.